

$$\begin{aligned} & \langle L \downarrow (q_g, +k_p) | L \downarrow (q_g, +k_p) \rangle \\ & = c_{L_L}^2(q_g) + c_{L_R}^2(q_g) = 1. \end{aligned} \quad (4)$$

Let us next consider the Hamiltonian H_k for a quark at the space axis, as expressed as,

$$H_{k_p} = H_{0,+k_p,+k_p} + H_{1,+k_p,-k_p}. \quad (5)$$

The energy for the right-handed chirality $|R \uparrow (q_g, +k_p)\rangle$ state can be estimated as

$$\begin{aligned} & \langle R \uparrow (q_g, +k_p) | H_{k_p} | R \uparrow (q_g, +k_p) \rangle \\ & = (2c_{R_R}^2(q_g) - 1) \mathcal{E}_{q_{m\infty},R} \\ & + 2c_{R_R}(q_g) \sqrt{1 - c_{R_R}^2(q_g)} \mathcal{E}_{q_{g\infty},R} \\ & = \varepsilon_{q_{m\infty},R}(q_g) + \varepsilon_{q_g,R}(q_g) \end{aligned} \quad (6)$$

where $\varepsilon_{q_{m\infty},R}(q_g)$ denotes the spin dipole magnetic energies for the right- $|R_R(+k_p)\rangle$ handed helicity element in the right-handed chirality $|R \uparrow (q_g, +k_p)\rangle$, and can be defined as

$$\varepsilon_{q_{m\infty},R}(q_g) = \langle R_R(+k_p) | H_{0,+k_p,+k_p} | R_R(+k_p) \rangle, \quad (7)$$

$$\begin{aligned} \varepsilon_{q_{m\infty},L}(q_g) & = \langle R_L(-k_p) | H_{0,+k_p,+k_p} | R_L(-k_p) \rangle \\ & = -\varepsilon_{q_{m\infty},R}(q_g) \end{aligned} \quad (8)$$

and the $\varepsilon_{q_{g\infty},R}$ denotes the mass energy originating from the interaction between the right- $|R_R(+k_p)\rangle$ and left- $|R_L(-k_p)\rangle$ handed helicity elements, which depends on the kind of particle, and related to the Higgs vacuum expectation value and Yukawa coupling constant [17],

$$\varepsilon_{q_{g\infty},R} = \langle R_R(+k_p) | H_{1,+k_p,-k_p} | R_L(-k_p) \rangle, \quad (9)$$

and the $\varepsilon_{q_g,R}(q_g)$ denotes the generated mass energy for the right-handed chirality $|R \uparrow (q_g, +k_p)\rangle$ state,

$$\varepsilon_{q_g,R}(q_g) = \varepsilon_{q_g,R,int.}(q_g) + \varepsilon_{q_g,R,ext.}(q_g)$$

$$= 2c_{R_R}(q_g) \sqrt{1 - c_{R_R}^2(q_g)} \mathcal{E}_{q_{g\infty},R}, \quad (10)$$

$$\begin{aligned} \varepsilon_{q_g,R,int.}(q_g) & = q_g c^2 \\ & \approx 2c_{R_R}(q_g) \sqrt{1 - c_{R_R}^2(q_g)} \mathcal{E}_{q_{g\infty},R}, \end{aligned} \quad (11)$$

$$\begin{aligned} \varepsilon_{q_g,R,ext.}(q_g) & = \varepsilon_{q_g,R, \text{gravitational field}}(q_g) \\ & = -G \frac{q_g}{r} \approx 0, \end{aligned} \quad (12)$$

and furthermore, $\varepsilon_{q_{m\infty},R}(q_g)$ denotes the spin dipole magnetic energy for the right-handed chirality state with mass q_g ,

$$\begin{aligned} \varepsilon_{q_{m\infty},R}(q_g) & = \varepsilon_{q_{m\infty},R,int.}(q_g) + \varepsilon_{q_{m\infty},R,ext.}(q_g) \\ & = \{c_{R_R}^2(q_g) - c_{R_L}^2(q_g)\} \mathcal{E}_{q_{m\infty},R} \\ & = (2c_{R_R}^2(q_g) - 1) \mathcal{E}_{q_{m\infty},R}, \end{aligned} \quad (13)$$

where

$$\varepsilon_{q_{m\infty},R,int.}(q_g) = 0, \quad (14)$$

$$\varepsilon_{q_{m\infty},R,ext.}(q_g) = (2c_{R_R}^2(q_g) - 1) \mathcal{E}_{q_{m\infty},R}. \quad (15)$$

Similar discussions can be made in the energy for the left-handed chirality $|L \downarrow (q_g, +k_p)\rangle$ states (Fig. 4),

$$\begin{aligned} & \langle L \downarrow (q_g, +k_p) | H_{k_p} | L \downarrow (q_g, +k_p) \rangle \\ & = (2c_{L_L}^2(q_g) - 1) \mathcal{E}_{q_{m\infty},L} \\ & + 2c_{L_L}(q_g) \sqrt{1 - c_{L_L}^2(q_g)} \mathcal{E}_{q_{g\infty},L} \\ & = \varepsilon_{q_{m\infty},L}(q_g) + \varepsilon_{q_g,L}(q_g) \end{aligned} \quad (16)$$

$$\varepsilon_{q_{m\infty},L}(q_g) = \langle L_L(+k_p) | H_{0,+k_p,+k_p} | L_L(+k_p) \rangle, \quad (17)$$

$$\begin{aligned} \varepsilon_{q_{m\infty},R}(q_g) & = \langle L_R(-k_p) | H_{0,+k_p,+k_p} | L_R(-k_p) \rangle \\ & = -\varepsilon_{q_{m\infty},L}(q_g) \end{aligned} \quad (18)$$

$$\varepsilon_{q_{g\infty},L} = \langle L_L(+k_p) | H_{1,+k_p,-k_p} | L_R(-k_p) \rangle, \quad (19)$$

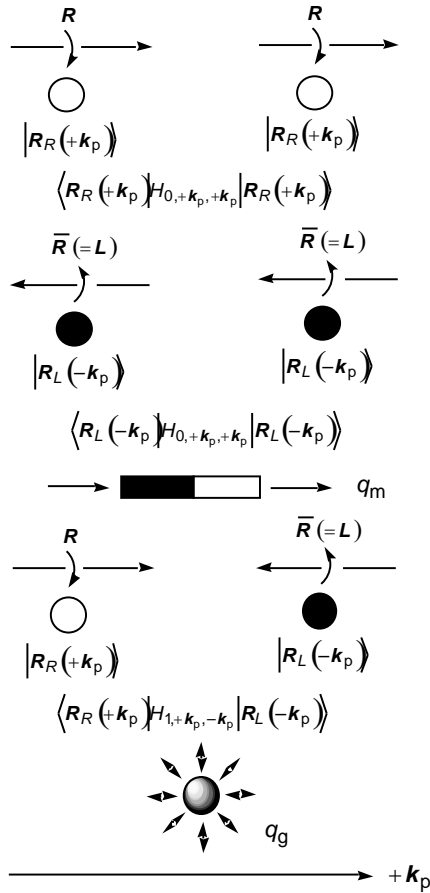


Fig. 2. Magnetic dipole moment and the mass in a right-handed particle at the particle spacetime axis. Opened and closed circles indicate the particle and antiparticle elements, respectively.

$$\begin{aligned} \varepsilon_{q_g, L}(q_g) &= \varepsilon_{q_g, L, \text{int.}}(q_g) + \varepsilon_{q_g, L, \text{ext.}}(q_g) \\ &= 2c_{L_L}(q_g) \sqrt{1 - c_{L_L}^2(q_g)} \mathcal{E}_{q_{g\infty, L}}, \end{aligned} \quad (20)$$

$$\begin{aligned} \varepsilon_{q_g, L, \text{int.}}(q_g) &= q_g c^2 \\ &\approx 2c_{L_L}(q_g) \sqrt{1 - c_{L_L}^2(q_g)} \mathcal{E}_{q_{g\infty, L}}, \end{aligned} \quad (21)$$

$$\begin{aligned} \varepsilon_{q_g, L, \text{ext.}}(q_g) &= \varepsilon_{q_g, L, \text{gravitational field}}(q_g) \\ &= -G \frac{q_g}{r} \approx 0, \end{aligned} \quad (22)$$

$$\begin{aligned} \varepsilon_{q_m, L}(q_g) &= \varepsilon_{q_m, L, \text{int.}}(q_g) + \varepsilon_{q_m, L, \text{ext.}}(q_g) \\ &= \{c_{L_L}^2(q_g) - c_{L_R}^2(q_g)\} \mathcal{E}_{q_{m\infty, L}} \\ &= (2c_{L_L}^2(q_g) - 1) \mathcal{E}_{q_{m\infty, L}}, \end{aligned} \quad (23)$$

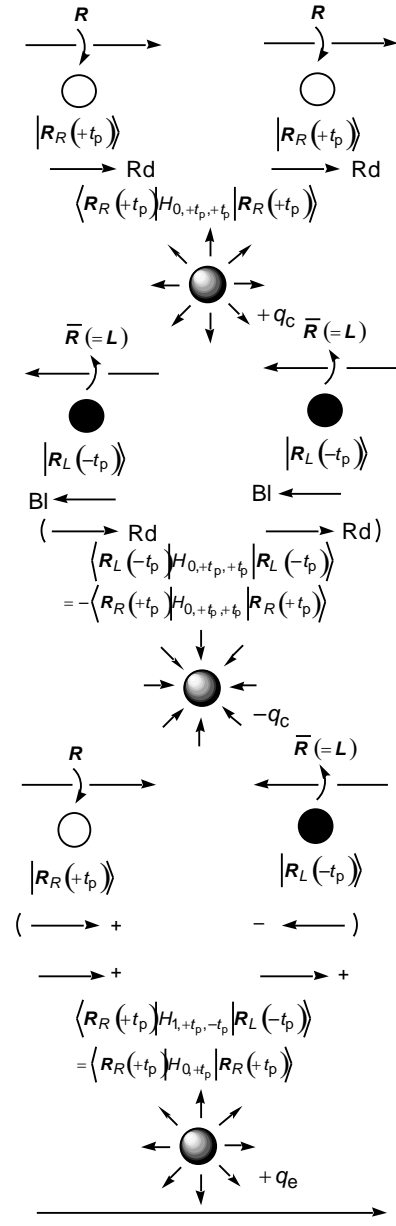


Fig. 3. Electric and color charges in a right-handed particle at the particle spacetime axis. Opened and closed circles indicate the particle and antiparticle elements, respectively.

$$\varepsilon_{q_m, L, \text{int.}}(q_g) = 0, \quad (24)$$

$$\varepsilon_{q_m, L, \text{ext.}}(q_g) = (2c_{L_L}^2(q_g) - 1) \mathcal{E}_{q_{m\infty, L}}. \quad (25)$$

2.2 Relationships between the Color Charge and Electric Charge (Electric Monopole) at Time Axis

Let us consider a quark in time axis, as shown in Figs. 3 and 5. We can consider that the spin state for a quark

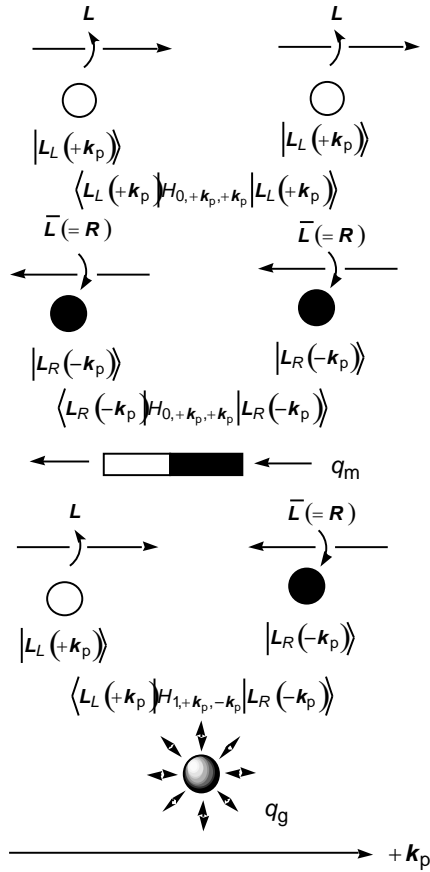


Fig. 4. Magnetic dipole moment and the mass in a left-handed particle at the particle spacetime axis. Opened and closed circles indicate the particle and antiparticle elements, respectively.

with electric charge q_e can be composed from the right-handed chirality $|R \uparrow(q_e, +t_p)\rangle$ or left-handed chirality $|L \downarrow(q_e, +t_p)\rangle$ elements (Fig. 1 (a)), defined as,

$$\begin{aligned}
 & |R \uparrow(q_e, +t_p)\rangle \\
 &= c_{R_R}(q_e) |R_R(+t_p)\rangle + c_{R_L}(q_e) |R_L(+t_a)\rangle \\
 &= c_{R_R}(q_e) |R_R(+t_p)\rangle + c_{R_L}(q_e) |R_L(-t_p)\rangle, \quad (26)
 \end{aligned}$$

$$\begin{aligned}
 & |L \downarrow(q_e, +t_p)\rangle \\
 &= c_{L_L}(q_e) |L_L(+t_p)\rangle + c_{L_R}(q_e) |L_R(+t_a)\rangle \\
 &= c_{L_L}(q_e) |L_L(+t_p)\rangle + c_{L_R}(q_e) |L_R(-t_p)\rangle, \quad (27)
 \end{aligned}$$

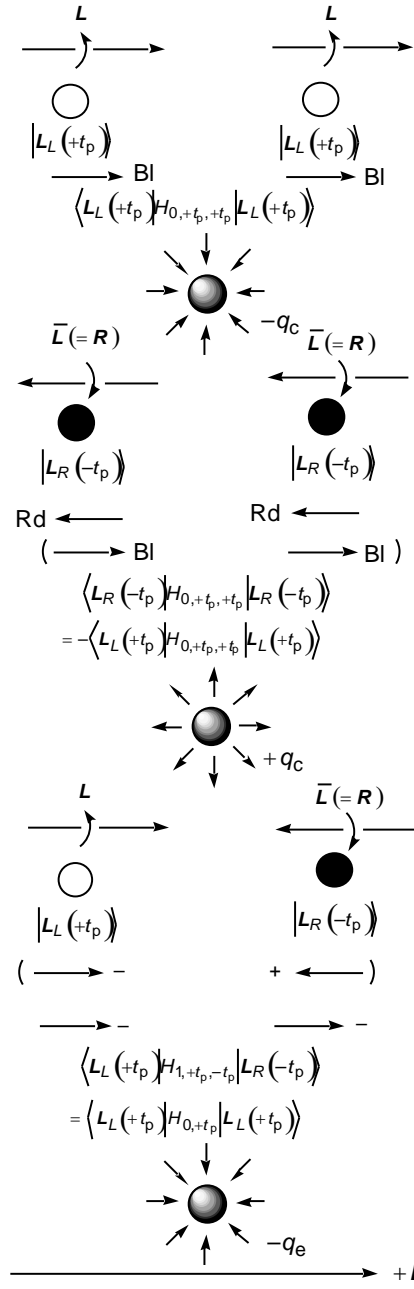


Fig. 5. Electric and color charges in a left-handed particle at the particle spacetime axis. Opened and closed circles indicate the particle and antiparticle elements, respectively.

where the $|R_R(+t_p)\rangle$ and $|R_L(-t_p)\rangle$ denote the right- and left-handed helicity elements in the right-handed chirality $|R \uparrow(q_e, +t_p)\rangle$ state, respectively, and the $|L_L(+t_p)\rangle$ and $|L_R(-t_p)\rangle$ denote the left- and right-handed helicity elements in the left-handed chirality

$|L \downarrow (q_e, +t_p)\rangle$ state, respectively. By considering the normalization of the $|R \uparrow (q_e, +t_p)\rangle$ and $|L \downarrow (q_e, +t_p)\rangle$ states, the relationships between the coefficients ($0 \leq c_{R_R}(q_e), c_{R_L}(q_e), c_{L_L}(q_e), c_{L_R}(q_e) \leq 1$) can be expressed as

$$\langle R \uparrow (q_e, +t_p) | R \uparrow (q_e, +t_p) \rangle = c_{R_R}^2(q_e) + c_{R_L}^2(q_e) = 1, \quad (28)$$

$$\langle L \downarrow (q_e, +t_p) | L \downarrow (q_e, +t_p) \rangle = c_{L_L}^2(q_e) + c_{L_R}^2(q_e) = 1. \quad (29)$$

Let us next consider the Hamiltonian H_t at the time axis, as expressed as,

$$H_{t_p} = H_{0,+t_p,+t_p} + H_{1,+t_p,-t_p}. \quad (30)$$

The energy for the right-handed chirality $|R \uparrow (q_e, +t_p)\rangle$ states can be estimated as

$$\begin{aligned} & \langle R \uparrow (q_e, +t_p) | H_{t_p} | R \uparrow (q_e, +t_p) \rangle \\ &= c_{R_R}^2(q_e) \varepsilon_{q_{\infty},R} + c_{R_L}^2(q_e) \varepsilon_{q_{\infty},L} \\ &+ 2c_{R_R}(q_e) \sqrt{1 - c_{R_R}^2(q_e)} \varepsilon_{q_{e\infty},R} \\ &= (2c_{R_R}^2(q_e) - 1) \varepsilon_{q_{e\infty},R} \\ &+ 2c_{R_R}(q_e) \sqrt{1 - c_{R_R}^2(q_e)} \varepsilon_{q_{e\infty},R} \\ &= \varepsilon_{q_c,R}(q_e) + \varepsilon_{q_e,R}(q_e), \end{aligned} \quad (31)$$

where $\varepsilon_{q_{\infty},R}$ and $\varepsilon_{q_{\infty},L}$ denote the energies for the right- $|R_R(+t_p)\rangle$ and left- $|R_L(+t_p)\rangle$ handed helicity elements in the right-handed chirality $|R \uparrow (q_e, +t_p)\rangle$, and can be defined as

$$\varepsilon_{q_{\infty},R} = \langle R_R(+t_p) | H_{0,+t_p,+t_p} | R_R(+t_p) \rangle, \quad (32)$$

$$\begin{aligned} \varepsilon_{q_{\infty},L} &= \langle R_L(-t_p) | H_{0,+t_p,+t_p} | R_L(-t_p) \rangle \\ &= -\langle R_R(+t_p) | H_{0,+t_p,+t_p} | R_R(+t_p) \rangle \\ &= -\varepsilon_{q_{\infty},R}, \end{aligned} \quad (33)$$

and the $\varepsilon_{q_{e\infty},R}$ denotes the electric monopole charge energy originating from the interaction between the right- $|R_R(+t_p)\rangle$ and left- $|R_L(-t_p)\rangle$ handed helicity elements at the time axis, which depends on the kind of particle,

$$\begin{aligned} \varepsilon_{q_{e\infty},R} &= \langle R_R(+t_p) | H_{1,+t_p,-t_p} | R_L(-t_p) \rangle \\ &= \langle R_R(+t_p) | H_{0,+t_p} | R_R(+t_p) \rangle, \end{aligned} \quad (34)$$

$$\begin{aligned} H_{1,+t_p,-t_p} | R_L(-t_p) \rangle &= H_{0,+t_p} | R_R(+t_p) \rangle \\ &= \varepsilon_{q_{e\infty},R} | R_R(+t_p) \rangle, \end{aligned} \quad (35)$$

and furthermore, $\varepsilon_{q_c,R}(q_e)$ denotes the color charge (q_c) energy for the right-handed chirality state with charge q_e ,

$$\begin{aligned} \varepsilon_{q_c,R}(q_e) &= \varepsilon_{q_c,R,int.}(q_e) + \varepsilon_{q_c,R,ext.}(q_e) \\ &= c_{R_R}^2(q_e) \varepsilon_{q_{\infty},R} + c_{R_L}^2(q_e) \varepsilon_{q_{\infty},L} \\ &= (2c_{R_R}^2(q_e) - 1) \varepsilon_{q_{\infty},R}, \end{aligned} \quad (36)$$

and the $\varepsilon_{q_e,R}(q_e)$ denotes the electric monopole charge energy for the right-handed chirality state with charge q_e ,

$$\begin{aligned} \varepsilon_{q_e,R}(q_e) &= \varepsilon_{q_e,R,int.}(q_e) + \varepsilon_{q_e,R,ext.}(q_e) \\ &= 2c_{R_R}(q_e) \sqrt{1 - c_{R_R}^2(q_e)} \varepsilon_{q_{e\infty},R}, \end{aligned} \quad (37)$$

$$\varepsilon_{q_e,R,int.}(q_e) = 0, \quad (38)$$

$$\begin{aligned} \varepsilon_{q_e,R,ext.}(q_e) &= \varepsilon_{q_e,R,electric\ field}(q_e) \\ &= 2c_{R_R}(q_e) \sqrt{1 - c_{R_R}^2(q_e)} \varepsilon_{q_{e\infty},R} \\ &= k_e q_e / r. \end{aligned} \quad (39)$$

Similar discussions can be made in the energy for the left-handed chirality $|L \downarrow (q_e, +t_p)\rangle$ states (Fig. 5),

$$\begin{aligned} & \langle L \downarrow (q_e, +t_p) | H_{t_p} | L \downarrow (q_e, +t_p) \rangle \\ &= c_{L_L}^2(q_e) \varepsilon_{q_{\infty},L} + c_{L_R}^2(q_e) \varepsilon_{q_{\infty},R} \\ &+ 2c_{L_L}(q_e) \sqrt{1 - c_{L_L}^2(q_e)} \varepsilon_{q_{e\infty},L} \\ &= (2c_{L_R}^2(q_e) - 1) \varepsilon_{q_{\infty},L} \\ &+ 2c_{L_L}(q_e) \sqrt{1 - c_{L_L}^2(q_e)} \varepsilon_{q_{e\infty},L} \\ &= \varepsilon_{q_c,L}(q_e) + \varepsilon_{q_e,L}(q_e), \end{aligned} \quad (40)$$

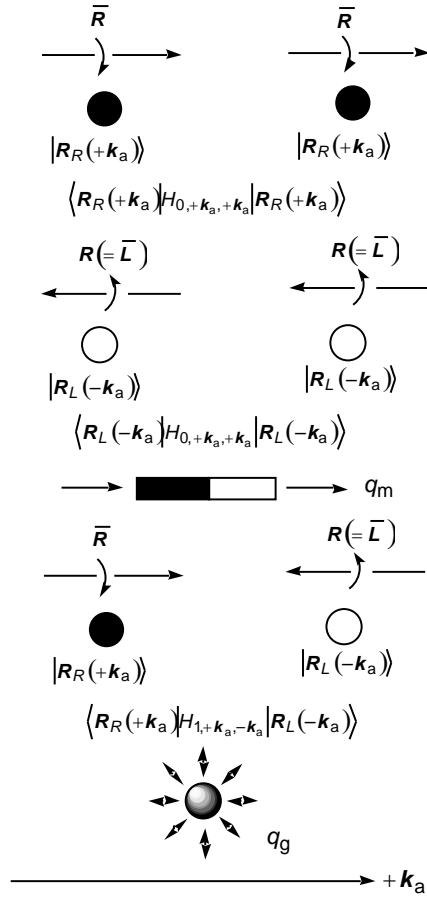


Fig. 6. Magnetic dipole moment and the mass in a right-handed antiparticle at the antiparticle spacetime axis. Opened and closed circles indicate the particle and antiparticle elements, respectively.

$$\varepsilon_{q_{\infty},L} = \langle L_L(+t_p) | H_{0,+t_p,+t_p} | L_L(+t_p) \rangle, \quad (41)$$

$$\begin{aligned} \varepsilon_{q_{\infty},R} &= \langle L_R(-t_p) | H_{0,+t_p,+t_p} | L_R(-t_p) \rangle \\ &= -\langle L_L(+t_p) | H_{0,+t_p,+t_p} | L_L(+t_p) \rangle \\ &= -\varepsilon_{q_{\infty},L}, \end{aligned} \quad (42)$$

$$\begin{aligned} \varepsilon_{q_{e\infty},L} &= \langle L_L(+t_p) | H_{1,+t_p,-t_p} | L_L(-t_p) \rangle \\ &= \langle L_L(+t_p) | H_{0,+t_p} | L_L(+t_p) \rangle, \end{aligned} \quad (43)$$

$$\begin{aligned} H_{1,+t_p,-t_p} | L_R(-t_p) \rangle &= H_{0,+t_p} | L_L(+t_p) \rangle \\ &= \varepsilon_{q_{e\infty},L} | L_L(+t_p) \rangle, \end{aligned} \quad (44)$$

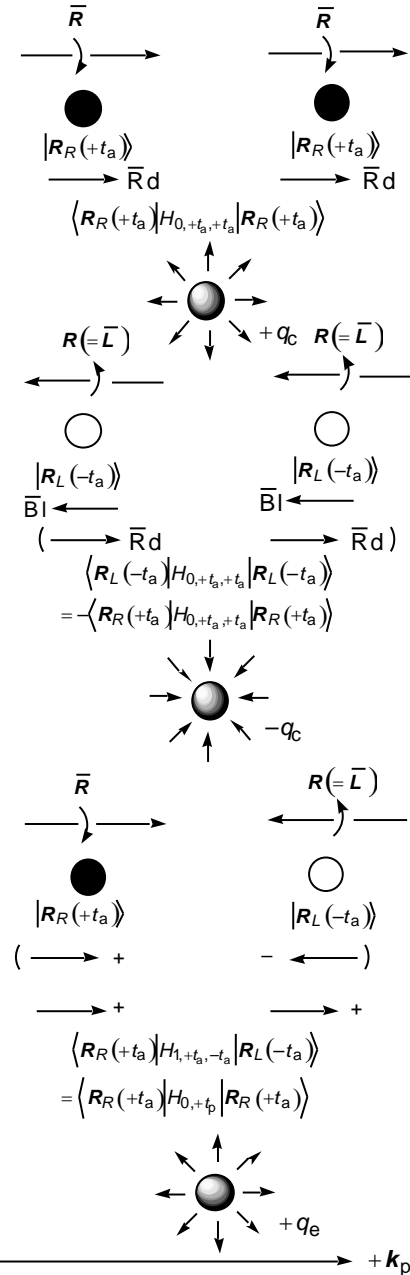


Fig. 7. Electric and color charges in a right-handed antiparticle at the antiparticle spacetime axis. Opened and closed circles indicate the particle and antiparticle elements, respectively.

$$\begin{aligned} \varepsilon_{q_e,L}(q_e) &= \varepsilon_{q_e,L,int.}(q_e) + \varepsilon_{q_e,L,ext.}(q_e) \\ &= c_{L_L}^2(q_e) \varepsilon_{q_{\infty},L} + c_{L_R}^2(q_e) \varepsilon_{q_{\infty},R} \\ &= (2c_{L_L}^2(q_e) - 1) \varepsilon_{q_{\infty},L}, \end{aligned} \quad (45)$$

$$\varepsilon_{q_e,L}(q_e) = \varepsilon_{q_e,L,int.}(q_e) + \varepsilon_{q_e,L,ext.}(q_e)$$

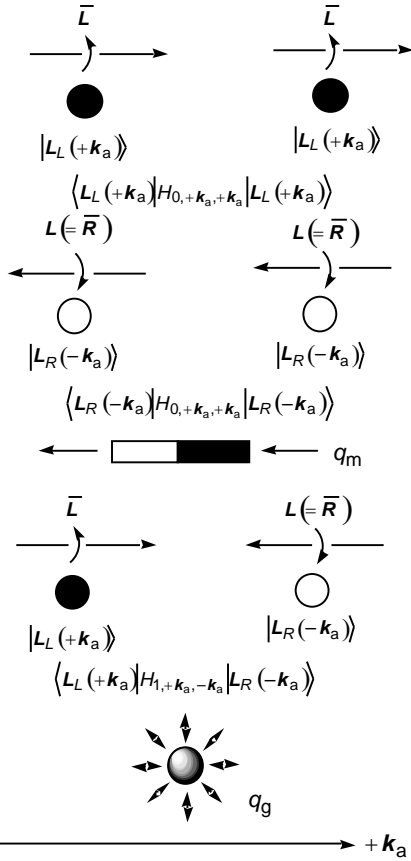


Fig. 8. Magnetic dipole moment and the mass in a left-handed antiparticle at the antiparticle spacetime axis. Opened and closed circles indicate the particle and antiparticle elements, respectively.

$$= 2c_{L_L}(q_e) \sqrt{1 - c_{L_L}^2(q_e)} \varepsilon_{q_{e\infty}, L} \quad (46)$$

$$\varepsilon_{q_e, L, \text{int.}}(q_e) = 0, \quad (47)$$

$$\begin{aligned} \varepsilon_{q_e, L, \text{ext.}}(q_e) &= \varepsilon_{q_e, L, \text{electric field}}(q_e) \\ &= 2c_{L_L}(q_e) \sqrt{1 - c_{L_L}^2(q_e)} \varepsilon_{q_{e\infty}, L} \\ &= k_e q_e / r. \end{aligned} \quad (48)$$

The quantized q_e values for the u , c , and t quarks are $+2/3$, those for the d , s , and b quarks are $-1/3$, those for the e , μ , and τ are -1 , and those for the ν_e , ν_μ , and ν_τ are ± 0 , at the particle time axis (t_p).

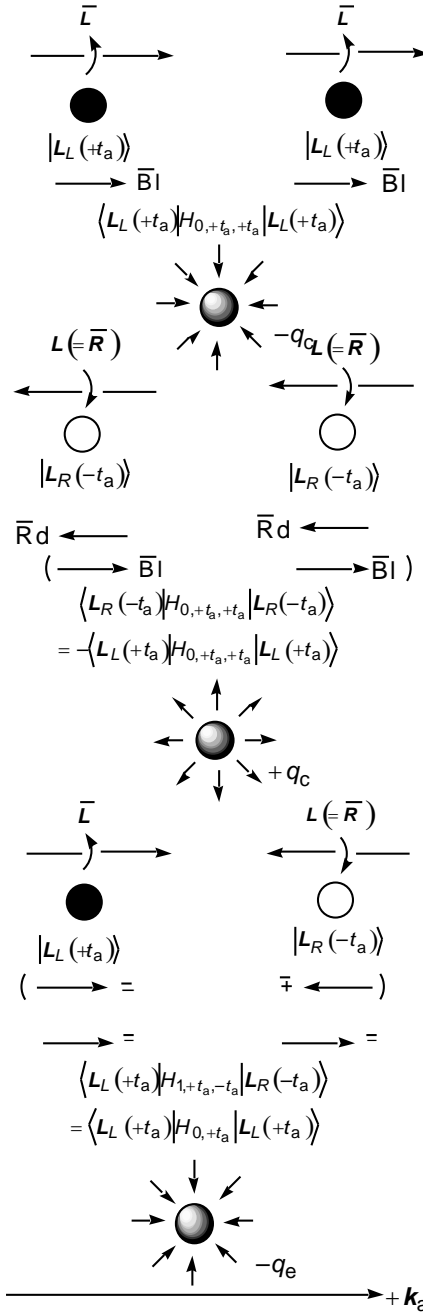


Fig. 9. Electric and color charges in a left-handed antiparticle at the antiparticle spacetime axis. Opened and closed circles indicate the particle and antiparticle elements, respectively.

3. Origin of the Magnetic Dipole Moment, Mass, Electric Charge, and Color Charge of an Antiparticle at the Antiparticle Spacetime Axis

Origin of the magnetic dipole moment, mass, electric charge, and color charge for the antiparticles at the antiparticle spacetime axis (Figs. 1 (b), 6–9) is equivalent to that for the particles at the particle spacetime axis (Figs.

2–5). The term “particle (antiparticle)” in the discussions of the particles at the particle spacetime axis should be changed to the term “antiparticle (particle)” in the discussions of the antiparticles at the antiparticle spacetime axis, and the subscript “p (a)” in the discussions of the particles at the particle spacetime axis should be changed to “a (p)” in the discussions of the antiparticles at the antiparticle spacetime axis., as shown in Figs. 6–9. The quantized q_e values for the \bar{u} , \bar{c} , and \bar{t} quarks are $+2/3$, those for the \bar{d} , \bar{s} , and \bar{b} quarks are $-1/3$, those for the \bar{e} , $\bar{\mu}$, and $\bar{\tau}$ are -1 , and those for the $\bar{\nu}_e$, $\bar{\nu}_\mu$, and $\bar{\nu}_\tau$ are ± 0 , at the antiparticle time axis (t_a).

4. Origin of the Magnetic Dipole Moment, Mass, Electric Charge, and Color Charge of an Antiparticle at the Particle Spacetime Axis

4.1 Relationships between the Spin Magnetic Dipole Moment and Mass at the Space Axis

Let us consider an antiparticle such as up and down antiquarks in three-dimensional space axis (Figs. 10–13). We can consider that the spin electronic state for an antiquark with massive charge q_g and momentum $-k_p$ can be composed from the right-handed chirality $\left| R \uparrow (q_g, -k_p) \right\rangle$ or left-handed chirality $\left| L \downarrow (q_g, -k_p) \right\rangle$ elements (Fig. 1 (c)), defined as,

$$\left| R \uparrow (q_g, -k_p) \right\rangle = c_{R_R}(q_g) \left| R_R(-k_p) \right\rangle + c_{R_L}(q_g) \left| R_L(+k_p) \right\rangle, \quad (49)$$

$$\left| L \downarrow (q_g, -k_p) \right\rangle = c_{L_L}(q_g) \left| L_L(-k_p) \right\rangle + c_{L_R}(q_g) \left| L_R(+k_p) \right\rangle, \quad (50)$$

where the $\left| R_R(-k_p) \right\rangle$ and $\left| R_L(+k_p) \right\rangle$ denote the right- and left-handed helicity elements in the right-handed chirality $\left| R \uparrow (q_g, -k_p) \right\rangle$ state, respectively, and the $\left| L_L(-k_p) \right\rangle$ and $\left| L_R(+k_p) \right\rangle$ denote the left- and right-handed helicity elements in the left-handed chirality $\left| L \downarrow (q_g, -k_p) \right\rangle$ state, respectively, at the space axis. By considering the normalizations of the $\left| R \uparrow (q_g, -k_p) \right\rangle$ and $\left| L \downarrow (q_g, -k_p) \right\rangle$ states, the relationships between the coefficients ($0 \leq c_{R_R}(q_g) c_{R_L}(q_g) c_{L_L}(q_g) c_{L_R}(q_g) \leq 1$) can be expressed as

$$\begin{aligned} & \left\langle R \uparrow (q_g, -k_p) \right| R \uparrow (q_g, -k_p) \rangle \\ & = c_{R_R}^2(q_g) + c_{R_L}^2(q_g) = 1, \end{aligned} \quad (51)$$

$$\begin{aligned} & \left\langle L \downarrow (q_g, -k_p) \right| L \downarrow (q_g, -k_p) \rangle \\ & = c_{L_L}^2(q_g) + c_{L_R}^2(q_g) = 1. \end{aligned} \quad (52)$$

Let us next consider the Hamiltonian H_k for an antiquark at the space axis, as expressed as,

$$H_{k_p} = H_{0,-k_p,-k_p} + H_{1,-k_p,+k_p}. \quad (53)$$

The energy for the right-handed chirality $\left| R \uparrow (q_g, -k_p) \right\rangle$ state can be estimated as

$$\begin{aligned} & \left\langle R \uparrow (q_g, -k_p) \right| H_{-k_p} \left| R \uparrow (q_g, -k_p) \right\rangle \\ & = \left(2c_{R_R}^2(q_g) - 1 \right) \varepsilon_{q_{m\infty},R} \\ & + 2c_{R_R}(q_g) \sqrt{1 - c_{R_R}^2(q_g)} \varepsilon_{q_{g\infty},R} \\ & = \varepsilon_{q_m,R}(q_g) + \varepsilon_{q_g,R}(q_g) \end{aligned} \quad (54)$$

where $\varepsilon_{q_{m\infty},R}(q_g)$ denotes the spin dipole magnetic energies for the right- $\left| R_R(-k_p) \right\rangle$ handed helicity element in the right-handed chirality $\left| R \uparrow (q_g, -k_p) \right\rangle$, and can be defined as

$$\varepsilon_{q_{m\infty},R}(q_g) = \left\langle R_R(-k_p) \right| H_{0,-k_p,-k_p} \left| R_R(-k_p) \right\rangle, \quad (55)$$

$$\varepsilon_{q_{m\infty},L}(q_g) = \left\langle R_L(+k_p) \right| H_{0,-k_p,-k_p} \left| R_L(+k_p) \right\rangle, \quad (56)$$

and the $\varepsilon_{q_{g\infty},R}$ denotes the mass energy originating from the interaction between the right- $\left| R_R(-k_p) \right\rangle$ and left- $\left| R_L(+k_p) \right\rangle$ handed helicity elements, which depends on the kind of antiparticle, and related to the Higgs vacuum expectation value and Yukawa coupling constant,

$$\varepsilon_{q_{g\infty},R} = \left\langle R_R(-k_p) \right| H_{1,-k_p,+k_p} \left| R_L(+k_p) \right\rangle, \quad (57)$$

and the $\varepsilon_{q_g,R}(q_g)$ denotes the generated mass energy for the right-handed chirality $\left| R \uparrow (q_g, -k_p) \right\rangle$ state,

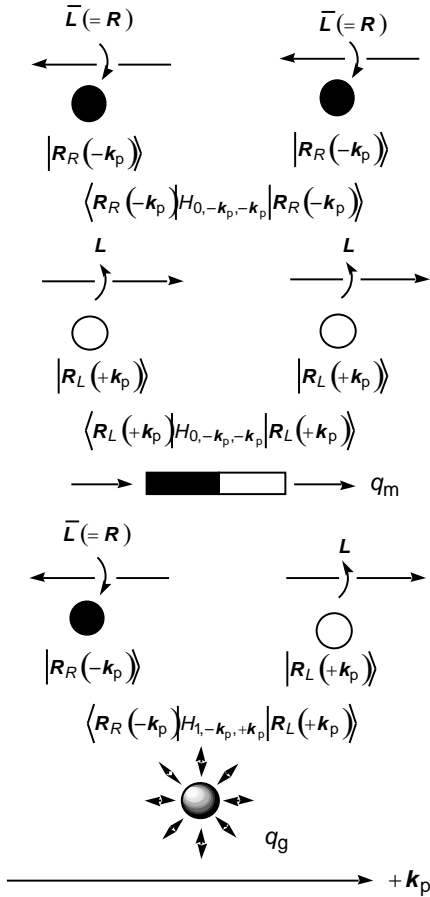


Fig. 10. Magnetic dipole moment and the mass in a right-handed antiparticle at the particle spacetime axis. Opened and closed circles indicate the particle and antiparticle elements, respectively.

$$\begin{aligned} \varepsilon_{q_g, R}(q_g) &= \varepsilon_{q_g, R, \text{int.}}(q_g) + \varepsilon_{q_g, R, \text{ext.}}(q_g) \\ &= 2c_{R_R}(q_g) \sqrt{1 - c_{R_R}^2(q_g)} \varepsilon_{q_{g\infty}, R}, \end{aligned} \quad (58)$$

$$\begin{aligned} \varepsilon_{q_g, R, \text{int.}}(q_g) &= q_g c^2 \\ &\approx 2c_{R_R}(q_g) \sqrt{1 - c_{R_R}^2(q_g)} \varepsilon_{q_{g\infty}, R}, \end{aligned} \quad (59)$$

$$\begin{aligned} \varepsilon_{q_g, R, \text{ext.}}(q_g) &= \varepsilon_{q_g, R, \text{gravitational field}}(q_g) \\ &= -G \frac{q_g}{r} \approx 0, \end{aligned} \quad (60)$$

and furthermore, $\varepsilon_{q_m, R}(q_g)$ denotes the spin dipole magnetic energy for the right-handed chirality state with mass q_g ,

$$\varepsilon_{q_m, R}(q_g) = \varepsilon_{q_m, R, \text{int.}}(q_g) + \varepsilon_{q_m, R, \text{ext.}}(q_g)$$

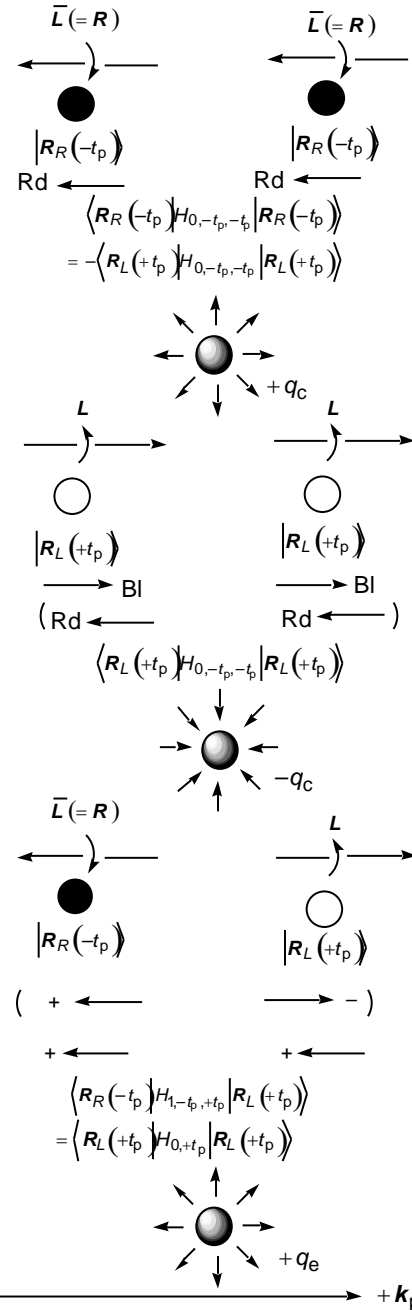


Fig. 11. Electric and color charges in a right-handed antiparticle at the particle spacetime axis. Opened and closed circles indicate the particle and antiparticle elements, respectively.

$$\begin{aligned} &= \{c_{R_R}^2(q_g) - c_{R_L}^2(q_g)\} \varepsilon_{q_{m\infty}, R} \\ &= (2c_{R_R}^2(q_g) - 1) \varepsilon_{q_{m\infty}, R}, \end{aligned} \quad (61)$$

where

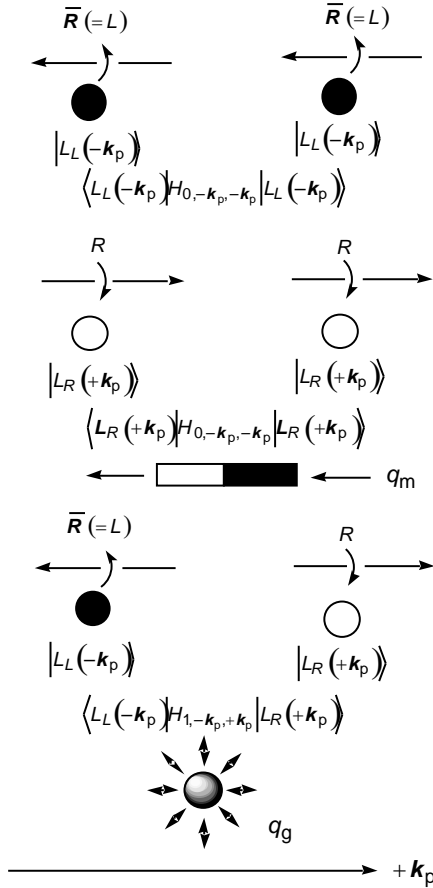


Fig. 12. Magnetic dipole moment and the mass in a left-handed antiparticle at the particle spacetime axis. Opened and closed circles indicate the particle and antiparticle elements, respectively.

$$\varepsilon_{q_m, R, \text{int.}}(q_g) = 0, \quad (62)$$

$$\varepsilon_{q_m, R, \text{ext.}}(q_g) = (2c_{L_R}^2(q_g) - 1) \varepsilon_{q_m, R}. \quad (63)$$

Similar discussions can be made in the energy for the left-handed chirality $|L \downarrow (q_g, -k_p)\rangle$ states (Fig. 12),

$$\begin{aligned} & \langle L \downarrow (q_g, -k_p) | H_{k_p} | L \downarrow (q_g, -k_p) \rangle \\ &= (2c_{L_L}^2(q_g) - 1) \varepsilon_{q_m, L} \\ &+ 2c_{L_L}(q_g) \sqrt{1 - c_{L_L}^2(q_g)} \varepsilon_{q_g, L} \\ &= \varepsilon_{q_m, L}(q_g) + \varepsilon_{q_g, L}(q_g) \end{aligned} \quad (64)$$

$$\varepsilon_{q_m, L}(q_g) = \langle L_L(-k_p) | H_{0, -k_p, -k_p} | L_L(-k_p) \rangle, \quad (65)$$

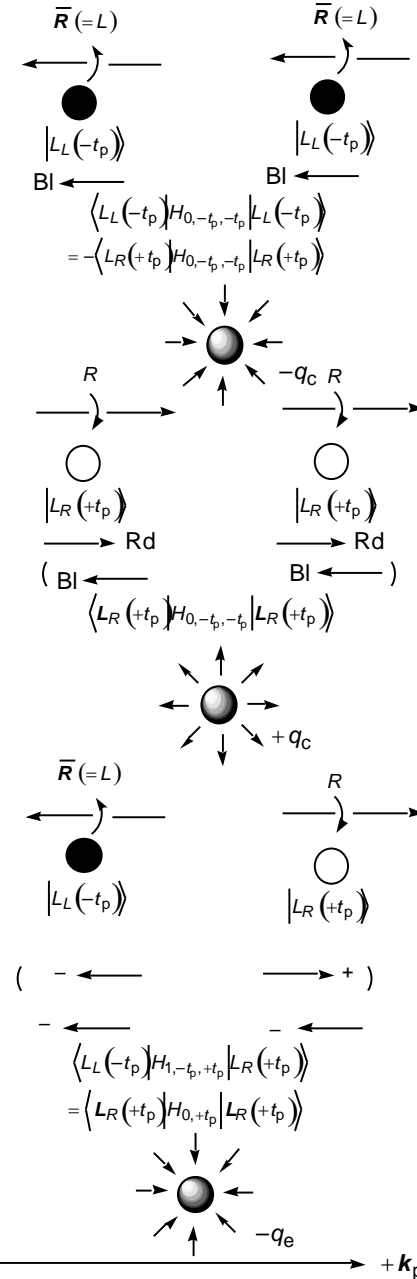


Fig. 13. Electric and color charges in a left-handed antiparticle at the particle spacetime axis. Opened and closed circles indicate the particle and antiparticle elements, respectively.

$$\begin{aligned} \varepsilon_{q_m, R}(q_g) &= \langle L_R(+k_p) | H_{0, -k_p, -k_p} | L_R(+k_p) \rangle \\ &= -\varepsilon_{q_m, L}(q_g) \end{aligned} \quad (66)$$

$$\varepsilon_{q_g, L} = \langle L_L(-k_p) | H_{1, -k_p, +k_p} | L_R(+k_p) \rangle, \quad (67)$$

$$\begin{aligned} \varepsilon_{q_g, L}(q_g) &= \varepsilon_{q_g, L, \text{int.}}(q_g) + \varepsilon_{q_g, L, \text{ext.}}(q_g) \\ &= 2c_{L_L}(q_g) \sqrt{1 - c_{L_L}^2(q_g)} \mathcal{E}_{q_{\infty}, L}, \end{aligned} \quad (68)$$

$$\begin{aligned} \varepsilon_{q_g, L, \text{int.}}(q_g) &= q_g c^2 \\ &\approx 2c_{L_L}(q_g) \sqrt{1 - c_{L_L}^2(q_g)} \mathcal{E}_{q_{\infty}, L}, \end{aligned} \quad (69)$$

$$\begin{aligned} \varepsilon_{q_g, L, \text{ext.}}(q_g) &= \varepsilon_{q_g, L, \text{gravitational field}}(q_g) \\ &= -G \frac{q_g}{r} \approx 0, \end{aligned} \quad (70)$$

$$\begin{aligned} \varepsilon_{q_m, L}(q_g) &= \varepsilon_{q_m, L, \text{int.}}(q_g) + \varepsilon_{q_m, L, \text{ext.}}(q_g) \\ &= \{c_{L_L}^2(q_g) - c_{L_R}^2(q_g)\} \mathcal{E}_{q_{\infty}, L} \\ &= (2c_{L_L}^2(q_g) - 1) \mathcal{E}_{q_{\infty}, L}, \end{aligned} \quad (71)$$

$$\varepsilon_{q_m, L, \text{int.}}(q_g) = 0, \quad (72)$$

$$\varepsilon_{q_m, L, \text{ext.}}(q_g) = (2c_{L_L}^2(q_g) - 1) \mathcal{E}_{q_{\infty}, L}. \quad (73)$$

4.2 Relationships between the Color Charge and Electric Charge (Electric Monopole) at Time Axis

Let us consider an antiquark in time axis, as shown in Figs. 11 and 13. We can consider that the spin state for an antiquark with electric charge q_e can be composed from the right-handed chirality $|\mathbf{R} \uparrow(q_e, -t_p)\rangle$ or left-handed chirality $|\mathbf{L} \downarrow(q_e, -t_p)\rangle$ elements (Fig. 1 (c)), defined as,

$$\begin{aligned} |\mathbf{R} \uparrow(q_e, -t_p)\rangle \\ = c_{R_R}(q_e) |\mathbf{R}_R(-t_p)\rangle + c_{R_L}(q_e) |\mathbf{R}_L(+t_p)\rangle, \end{aligned} \quad (74)$$

$$\begin{aligned} |\mathbf{L} \downarrow(q_e, -t_p)\rangle \\ = c_{L_L}(q_e) |\mathbf{L}_L(-t_p)\rangle + c_{L_R}(q_e) |\mathbf{L}_R(+t_p)\rangle, \end{aligned} \quad (75)$$

where the $|\mathbf{R}_R(-t_p)\rangle$ and $|\mathbf{R}_L(+t_p)\rangle$ denote the right- and left-handed helicity elements in the right-handed chirality $|\mathbf{R} \uparrow(q_e, -t_p)\rangle$ state, respectively, and the $|\mathbf{L}_L(-t_p)\rangle$ and $|\mathbf{L}_R(+t_p)\rangle$ denote the left- and right-handed helicity elements in the left-handed chirality

$|\mathbf{L} \downarrow(q_e, -t_p)\rangle$ state, respectively. By considering the normalization of the $|\mathbf{R} \uparrow(q_e, -t_p)\rangle$ and $|\mathbf{L} \downarrow(q_e, -t_p)\rangle$ states, the relationships between the coefficients ($0 \leq c_{R_R}(q_e), c_{R_L}(q_e), c_{L_L}(q_e), c_{L_R}(q_e) \leq 1$) can be expressed as

$$\langle \mathbf{R} \uparrow(q_e, -t_p) | \mathbf{R} \uparrow(q_e, -t_p) \rangle = c_{R_R}^2(q_e) + c_{R_L}^2(q_e) = 1, \quad (76)$$

$$\langle \mathbf{L} \downarrow(q_e, -t_p) | \mathbf{L} \downarrow(q_e, -t_p) \rangle = c_{L_L}^2(q_e) + c_{L_R}^2(q_e) = 1. \quad (77)$$

Let us next consider the Hamiltonian H_t at the time axis, as expressed as,

$$H_{t_p} = H_{0, -t_p, -t_p} + H_{1, -t_p, +t_p}. \quad (78)$$

The energy for the right-handed chirality $|\mathbf{R} \uparrow(q_e, -t_p)\rangle$ states can be estimated as

$$\begin{aligned} \langle \mathbf{R} \uparrow(q_e, -t_p) | H_{t_p} | \mathbf{R} \uparrow(q_e, -t_p) \rangle \\ = c_{R_R}^2(q_e) \varepsilon_{q_{\infty}, R} + c_{R_L}^2(q_e) \varepsilon_{q_{\infty}, L} \\ + 2c_{R_R}(q_e) \sqrt{1 - c_{R_R}^2(q_e)} \varepsilon_{q_{\infty}, R} \\ = (2c_{R_R}^2(q_e) - 1) \varepsilon_{q_{\infty}, R} \\ + 2c_{R_R}(q_e) \sqrt{1 - c_{R_R}^2(q_e)} \varepsilon_{q_{\infty}, R} \\ = \varepsilon_{q_e, R}(q_e) + \varepsilon_{q_e, R}(q_e), \end{aligned} \quad (79)$$

where $\varepsilon_{q_{\infty}, R}$ and $\varepsilon_{q_{\infty}, L}$ denote the energies for the right- $|\mathbf{R}_R(-t_p)\rangle$ and left- $|\mathbf{R}_L(+t_p)\rangle$ handed helicity elements in the right-handed chirality $|\mathbf{R} \uparrow(q_e, -t_p)\rangle$, and can be defined as

$$\begin{aligned} \varepsilon_{q_{\infty}, R} &= \langle \mathbf{R}_R(-t_p) | H_{0, -t_p, -t_p} | \mathbf{R}_R(-t_p) \rangle \\ &= -\langle \mathbf{R}_L(+t_p) | H_{0, -t_p, -t_p} | \mathbf{R}_L(+t_p) \rangle, \end{aligned} \quad (80)$$

$$\begin{aligned} \varepsilon_{q_{\infty}, L} &= \langle \mathbf{R}_L(+t_p) | H_{0, -t_p, -t_p} | \mathbf{R}_L(+t_p) \rangle \\ &= -\varepsilon_{q_{\infty}, R}, \end{aligned} \quad (81)$$

and the $\varepsilon_{q_{e\infty},R}$ denotes the electric monopole charge energy originating from the interaction between the right- $\left|R_R(-t_p)\right\rangle$ and left- $\left|R_L(+t_p)\right\rangle$ handed helicity elements at the time axis, which depends on the kind of antiparticle,

$$\begin{aligned} \varepsilon_{q_{e\infty},R} &= \left\langle R_R(-t_p) \left| H_{1,-t_p,+t_p} \right| R_L(+t_p) \right\rangle \\ &= \left\langle R_L(+t_p) \left| H_{0,+t_p} \right| R_L(+t_p) \right\rangle, \end{aligned} \quad (82)$$

$$\begin{aligned} \left\langle R_R(-t_p) \left| H_{1,-t_p,+t_p} \right. \right. &= \left. \left. \left\langle R_L(+t_p) \left| H_{0,+t_p} \right. \right. \right. \\ &= \varepsilon_{q_{e\infty},R} \left\langle R_L(+t_p) \right. \end{aligned} \quad (83)$$

and furthermore, $\varepsilon_{q_c,R}(q_e)$ denotes the color charge (q_c) energy for the right-handed chirality state with charge q_e ,

$$\begin{aligned} \varepsilon_{q_c,R}(q_e) &= \varepsilon_{q_c,R,int.}(q_e) + \varepsilon_{q_c,R,ext.}(q_e) \\ &= c_{R_R}^2(q_e) \varepsilon_{q_{c\infty},R} + c_{R_L}^2(q_e) \varepsilon_{q_{c\infty},L} \\ &= (2c_{R_R}^2(q_e) - 1) \varepsilon_{q_{c\infty},R}, \end{aligned} \quad (84)$$

and the $\varepsilon_{q_e,R}(q_e)$ denotes the electric monopole charge energy for the right-handed chirality state with charge q_e ,

$$\begin{aligned} \varepsilon_{q_e,R}(q_e) &= \varepsilon_{q_e,R,int.}(q_e) + \varepsilon_{q_e,R,ext.}(q_e) \\ &= 2c_{R_R}(q_e) \sqrt{1 - c_{R_R}^2(q_e)} \varepsilon_{q_{e\infty},R}, \end{aligned} \quad (85)$$

$$\varepsilon_{q_e,R,int.}(q_e) = 0, \quad (86)$$

$$\begin{aligned} \varepsilon_{q_e,R,ext.}(q_e) &= \varepsilon_{q_e,R,electric\ field}(q_e) \\ &= 2c_{R_R}(q_e) \sqrt{1 - c_{R_R}^2(q_e)} \varepsilon_{q_{e\infty},R} \\ &= k_e q_e / r. \end{aligned} \quad (87)$$

Similar discussions can be made in the energy for the left-handed chirality $\left|L\downarrow(q_e, -t_p)\right\rangle$ states,

$$\begin{aligned} &\left\langle L\downarrow(q_e, -t_p) \left| H_{t_p} \right| L\downarrow(q_e, -t_p) \right\rangle \\ &= c_{L_L}^2(q_e) \varepsilon_{q_{c\infty},L} + c_{L_R}^2(q_e) \varepsilon_{q_{c\infty},R} \\ &+ 2c_{L_L}(q_e) \sqrt{1 - c_{L_L}^2(q_e)} \varepsilon_{q_{e\infty},L} \\ &= (2c_{L_R}^2(q_e) - 1) \varepsilon_{q_{c\infty},L} \\ &+ 2c_{L_L}(q_e) \sqrt{1 - c_{L_L}^2(q_e)} \varepsilon_{q_{e\infty},L} \end{aligned}$$

$$= \varepsilon_{q_c,L}(q_e) + \varepsilon_{q_e,L}(q_e), \quad (88)$$

$$\varepsilon_{q_{c\infty},L} = -\left\langle L_R(+t_p) \left| H_{0,-t_p,-t_p} \right| L_R(+t_p) \right\rangle, \quad (89)$$

$$\begin{aligned} \varepsilon_{q_{c\infty},R} &= \left\langle L_R(+t_p) \left| H_{0,-t_p,-t_p} \right| L_R(+t_p) \right\rangle \\ &= -\varepsilon_{q_{c\infty},L}, \end{aligned} \quad (90)$$

$$\begin{aligned} \varepsilon_{q_{e\infty},L} &= \left\langle L_L(-t_p) \left| H_{1,-t_p,+t_p} \right| L_R(+t_p) \right\rangle \\ &= \left\langle L_R(+t_p) \left| H_{0,+t_p} \right| L_R(+t_p) \right\rangle, \end{aligned} \quad (91)$$

$$\begin{aligned} \left\langle L_L(-t_p) \left| H_{1,-t_p,+t_p} \right. \right. &= \left. \left. \left\langle L_R(+t_p) \left| H_{0,+t_p} \right. \right. \right. \\ &= \varepsilon_{q_{e\infty},L} \left\langle L_R(+t_p) \right. \end{aligned} \quad (92)$$

$$\begin{aligned} \varepsilon_{q_c,L}(q_e) &= \varepsilon_{q_c,L,int.}(q_e) + \varepsilon_{q_c,L,ext.}(q_e) \\ &= c_{L_L}^2(q_e) \varepsilon_{q_{c\infty},L} + c_{L_R}^2(q_e) \varepsilon_{q_{c\infty},R} \\ &= (2c_{L_L}^2(q_e) - 1) \varepsilon_{q_{c\infty},L}, \end{aligned} \quad (93)$$

$$\begin{aligned} \varepsilon_{q_e,L}(q_e) &= \varepsilon_{q_e,L,int.}(q_e) + \varepsilon_{q_e,L,ext.}(q_e) \\ &= 2c_{L_L}(q_e) \sqrt{1 - c_{L_L}^2(q_e)} \varepsilon_{q_{e\infty},L}, \end{aligned} \quad (94)$$

$$\varepsilon_{q_e,L,int.}(q_e) = 0, \quad (95)$$

$$\begin{aligned} \varepsilon_{q_e,L,ext.}(q_e) &= \varepsilon_{q_e,L,electric\ field}(q_e) \\ &= 2c_{L_L}(q_e) \sqrt{1 - c_{L_L}^2(q_e)} \varepsilon_{q_{e\infty},L} \\ &= k_e q_e / r. \end{aligned} \quad (96)$$

The quantized q_e values for the \bar{u} , \bar{c} , and \bar{t} antiquarks are $-2/3$, those for the \bar{d} , \bar{s} , and \bar{b} antiquarks are $+1/3$, those for the \bar{e} , $\bar{\mu}$, and $\bar{\tau}$ are $+1$, and those for the $\bar{\nu}_e$, $\bar{\nu}_\mu$, and $\bar{\nu}_\tau$ are ± 0 , at the particle time axis (t_p).

5. Relationships between the Spin Magnetic Dipole Moment, Massive Charge, Electric Monopole Charge, and Color Charge; Particles at the Particle Spacetime Axis

5.1 Spin Magnetic Dipole Moment

The energies for the spin magnetic dipole moment for the $\left|R\uparrow(q_g, +k_p)\right\rangle$ state can be expressed as Eq. (13).

At the time of the Big Bang, the $\varepsilon_{q_m,R}(q_g)$ and

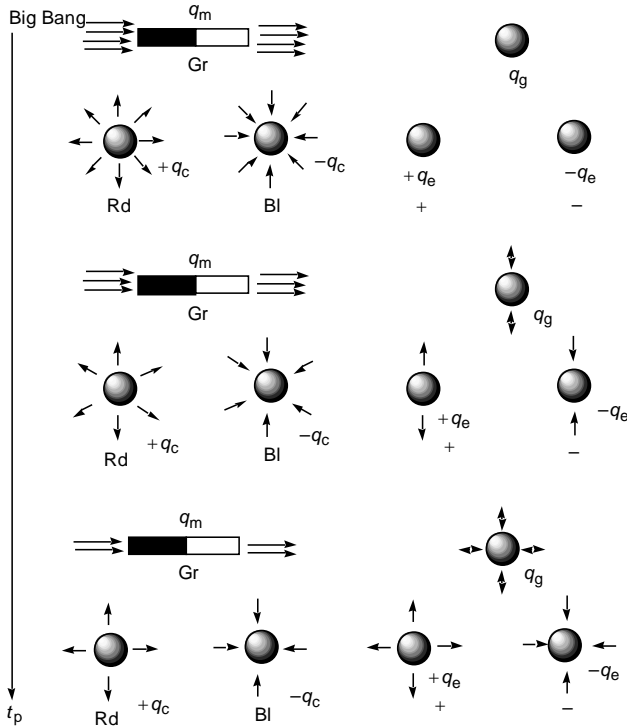


Fig. 14. Intensity of the magnetic dipole moment, gravitational field, electric field, and color field as a function of time.

$\varepsilon_{q_m, L}(q_g)$ values were the maximum (Fig. 14). That is, there was no mixture between the right- $|R_R(+k_p)\rangle$ and left- $|R_L(-k_p)\rangle (= |R_L(+k_a)\rangle)$ handed helicity elements, and thus the spin magnetic dipole moment was the largest at the Big Bang. In other words, the mass (infinitesimal electric dipole charge) and electric monopole charge were not generated at that time. However, since temperatures immediately decreased after Big Bang, because of any origin (i.e., Higgs boson, broken symmetry of chirality etc.), the mixture between the right- $|R_R(+k_p)\rangle$ and left- $|R_L(-k_p)\rangle$ handed helicity elements has begun to occur. The mixture between the right- $|R_R(+k_p)\rangle$ and left- $|R_L(-k_p)\rangle$ handed helicity elements increases with an increase in time (with a decrease in the $c_{R_R}(q_g)$ value). Similar discussions can be made in the $|L\downarrow(q_g, +k_p)\rangle$ state.

We can see from Figs. 2 and 4 that the $\varepsilon_{q_m, R}(q_g)$ and $\varepsilon_{q_m, L}(q_g)$ values are not equivalent in the space axis.

The total chirality and momentum in the $\langle R_R(+k_p) | H_{0,+k_p,+k_p} | R_R(+k_p) \rangle$ and $\langle L_L(+k_p) | H_{0,+k_p,+k_p} | L_L(+k_p) \rangle$ terms in the both $|R\uparrow(q_g, +k_p)\rangle$ and $|L\downarrow(q_g, +k_p)\rangle$ states are not zero. This is the reason why the number of elements for magnetic spin dipole moments is two, and thus there are attractive and repulsive forces between two magnetic dipole moments.

The spin magnetic dipole energy is proportional to the $\langle R_R(+k_p) | H_{0,+k_p,+k_p} | R_R(+k_p) \rangle$ and $\langle R_L(-k_p) | H_{0,+k_p,+k_p} | R_L(-k_p) \rangle$ values, and the $\langle L_L(+k_p) | H_{0,+k_p,+k_p} | L_L(+k_p) \rangle$ and $\langle L_R(-k_p) | H_{0,+k_p,+k_p} | L_R(-k_p) \rangle$ values (Figs. 2 and 4).

These values are different between the kinds of particles and antiparticles. This is the reason why we cannot theoretically predict the intensity of the spin magnetic dipole moment for each particle or antiparticle. In summary, because of the $\langle R_R(+k_p) | H_{0,+k_p,+k_p} | R_R(+k_p) \rangle$ and $\langle L_L(+k_p) | H_{0,+k_p,+k_p} | L_L(+k_p) \rangle$ terms, originating from the finite right- and left-handed helicity elements, respectively, the magnetic dipole field goes from the infinitesimal source point to infinitesimal sink point at finite space axis. This is the reason why the path of the magnetic dipole field is like loop (source-sink)-type, as shown in Figs. 2 and 4.

It should be noted that the strength of the spin magnetic dipole moment depends on the direction at the space axis. That is, the strength of the spin magnetic dipole moment can change, according to the spatial environment. This is because the spin magnetic dipole moment can be defined as the difference between the right- $\langle R_R(+k_p) | H_{0,+k_p,+k_p} | R_R(+k_p) \rangle$ and left-handed $\langle R_L(-k_p) | H_{0,+k_p,+k_p} | R_L(-k_p) \rangle$ angular momentum elements (space $k_p (\neq 0)$ dependent ($+k_p$ or $-k_p$)). That is, we can consider that the spin magnetic dipole moments are not rigid with respect to the spatial environment. We can consider that the spin magnetic dipole moment observed in our real world can be defined as the difference of the spin angular momentum between the components of wave function for the right- (left-) handed particle and the right- (left-) handed antiparticle, as shown in Figs. 2, 4, 6, 8, 10, and 12.

If we observe the magnetic dipole moment in large enough range and time ($\Delta r \gg 0, \Delta t \gg 0$), we would observe average $\varepsilon_{q_m, R, obs. \Delta r, t \gg 0}$ and $\varepsilon_{q_m, L, obs. \Delta r, t \gg 0}$ values originating from both the $\langle \mathbf{R}_R(+k_p) | H_{0,+k_p,+k_p} | \mathbf{R}_R(+k_p) \rangle$ and $\langle \mathbf{R}_L(-k_p) | H_{0,+k_p,+k_p} | \mathbf{R}_L(-k_p) \rangle$ terms, and both the $\langle \mathbf{L}_L(+k_p) | H_{0,+k_p,+k_p} | \mathbf{L}_L(+k_p) \rangle$ and $\langle \mathbf{L}_R(-k_p) | H_{0,+k_p,+k_p} | \mathbf{L}_R(-k_p) \rangle$ terms, respectively,

$$\varepsilon_{q_m, R, obs. \Delta r, t \gg 0} = (2c_{R_R}^2(q_g) - 1) \varepsilon_{q_{m\infty}, R} \quad (97)$$

$$\varepsilon_{q_m, L, obs. \Delta r, t \gg 0} = (2c_{L_L}^2(q_g) - 1) \varepsilon_{q_{m\infty}, L} \quad (98)$$

On the other hand, if we observe the magnetic dipole moment in small enough range and time ($\Delta r \approx 0, \Delta t \approx 0$), we would observe various $\varepsilon_{q_m, R, obs. \Delta r, t \approx 0}$ values originating from only the $\langle \mathbf{R}_R(+k_p) | H_{0,+k_p,+k_p} | \mathbf{R}_R(+k_p) \rangle$, or $\langle \mathbf{R}_L(-k_p) | H_{0,+k_p,+k_p} | \mathbf{R}_L(-k_p) \rangle$, or other combinations between them, and from only the $\langle \mathbf{L}_L(+k_p) | H_{0,+k_p,+k_p} | \mathbf{L}_L(+k_p) \rangle$, or $\langle \mathbf{L}_R(-k_p) | H_{0,+k_p,+k_p} | \mathbf{L}_R(-k_p) \rangle$, or other combinations between them,

$$\begin{aligned} \varepsilon_{q_m, R, obs. \Delta r, t \approx 0} &= \varepsilon_{q_{m\infty}, R} \\ &= \varepsilon_{q_{m\infty}, L} \\ &= \text{etc.} \end{aligned} \quad (99)$$

$$\begin{aligned} \varepsilon_{q_m, L, obs. \Delta r, t \approx 0} &= \varepsilon_{q_{m\infty}, L} \\ &= \varepsilon_{q_{m\infty}, R} \\ &= \text{etc.} \end{aligned} \quad (100)$$

That is, if we observe the magnetic dipole moment in large enough range and time (i.e., the uncertainty of the position and time is very large ($\Delta r \gg 0, t \gg 0$)), we would observe the average $\varepsilon_{q_m, R, obs. \Delta r, t \gg 0}$ and $\varepsilon_{q_m, L, obs. \Delta r, t \gg 0}$ values with very small uncertainty in momentum and energy ($\Delta k \approx 0, \Delta E \approx 0$), as usual. On the other hand, if we observe the magnetic dipole moment in small enough range and time (i.e., the uncertainty of the position and time is very small ($\Delta r \approx 0, \Delta t \approx 0$)), we would observe the various $\varepsilon_{q_m, R, obs. \Delta r, t \approx 0}$ and

$\varepsilon_{q_m, L, obs. \Delta r, t \approx 0}$ values with very large uncertainty in momentum and energy ($\Delta k \gg 0, \Delta E \gg 0$). This can be related to the Heisenberg's uncertainty principle.

5.2 Mass (Infinitesimal Electric (and Magnetic) Dipole Charge)

The mass energy $\varepsilon_{q_g, R}(q_g)$ for the right-handed chirality $|\mathbf{R} \uparrow(q_g, +k_p)\rangle$ element can be defined as Eq. (10). At the time of the Big Bang, the $\varepsilon_{q_g, R}(q_g)$ value was the minimum ($c_{R_R}(q_g) = 1$) (Fig. 14). That is, there was no mixture between the right- $|\mathbf{R}_R(+k_p)\rangle$ and left- $|\mathbf{R}_L(-k_p)\rangle$ handed helicity elements, and thus the mass energy was zero at the Big Bang. In other words, the mass was not generated at that time. However, after that, temperature significantly decreased, and thus because of any origin (i.e., Higgs boson, broken symmetry of chirality etc.), the mixture between the right- $|\mathbf{R}_R(+k_p)\rangle$ and left- $|\mathbf{R}_L(-k_p)\rangle$ handed helicity elements has begun to occur. The mixture between the right- $|\mathbf{R}_R(+k_p)\rangle$ and left- $|\mathbf{R}_L(-k_p)\rangle$ handed helicity elements increases with an increase in time (with a decrease in the $c_{R_R}(q_g)$ value). Similar discussions can be made in the $|\mathbf{L} \downarrow(q_g, +k_p)\rangle$ state.

The mass energy is proportional to the $\langle \mathbf{R}_R(+k_p) | H_{1,+k_p,-k_p} | \mathbf{R}_L(-k_p) \rangle$ and $\langle \mathbf{L}_L(+k_p) | H_{1,+k_p,-k_p} | \mathbf{L}_R(-k_p) \rangle$ values (Figs. 2 and 4). These values are different between the kinds of particles. This is the reason why we do not theoretically predict the mass for each particle or antiparticle.

We can see from Figs. 2 and 4 that the $\varepsilon_{q_g, R}(q_g)$ and $\varepsilon_{q_g, L}(q_g)$ values are equivalent in the space axis. The total chirality and momentum in the $\langle \mathbf{R}_R(+k_p) | H_{1,+k_p,-k_p} | \mathbf{R}_L(-k_p) \rangle$ and $\langle \mathbf{L}_L(+k_p) | H_{1,+k_p,-k_p} | \mathbf{L}_R(-k_p) \rangle$ terms in the both $|\mathbf{R} \uparrow(q_g, +k_p)\rangle$ and $|\mathbf{L} \downarrow(q_g, +k_p)\rangle$ states are zero. We can consider that the mass is generated by the mixture of the right- $|\mathbf{R}_R(+k_p)\rangle$ and left- $|\mathbf{R}_L(-k_p)\rangle$ handed helicity elements at the space axis. In the real world we

live, the reversible process ($-k_p$) can be possible in the space axis while the reversible process ($-t_p$) cannot be possible in the time axis (irreversible). This is the reason why the number of elements for mass is only one, and thus there is only attractive force between two masses.

In summary, because of the $\langle R_R(+k_p) | H_{1,+k_p,-k_p} | R_L(-k_p) \rangle$ and $\langle L_L(+k_p) | H_{1,+k_p,-k_p} | L_R(-k_p) \rangle$ terms, originating from the cancellation of the right- and left-handed helicity elements at space axis, the gravitational fields only spring out from the infinitesimal source point (or comes into the infinitesimal sink point) to (from) any direction in the space axis.

On the other hand, the total chirality and momentum in the $\langle R_R(+k_p) | H_{1,+k_p,-k_p} | R_L(-k_p) \rangle$ and $\langle L_L(+k_p) | H_{1,+k_p,-k_p} | L_R(-k_p) \rangle$ states are zero not because of the intrinsic zero value but because of the cancellation of the large right- and left-handed helicity elements, which are the origin of the spin magnetic moment and the electric charge. Therefore, there is a possibility that the external potential energy ($\varepsilon_{q_g,ext.,R}(q_g)$ and $\varepsilon_{q_g,ext.,L}(q_g)$) for the $\langle R_R(+k_p) | H_{1,+k_p,-k_p} | R_L(-k_p) \rangle$ and $\langle L_L(+k_p) | H_{1,+k_p,-k_p} | L_R(-k_p) \rangle$ states can be very small but finite values (fluctuated and induced polarization effects). Therefore, the distortion of the spacetime axes can occur. That is, we can consider that the gravity can be considered to be the residual electromagnetic forces [14]. Such fluctuation originates from the fact that the q_g value is decided under the very small uncertainty of the position ($\Delta r \approx 0$) and time ($\Delta t \approx 0$), and thus the uncertainty of the momentum ($\Delta k \gg 0$) and energy ($\Delta E \gg 0$) is very large (Heisenberg's uncertainty principle).

Most of extremely large energy generated at the time of the Big Bang has been stored in the particle and antiparticle as a large potential rest energy, and only small part of it is now used as very small gravitational energy. This is the reason why the gravity is much smaller than other three forces.

It should be noted that the strength of the massive charge is observed to be always constant, and not to depend on the direction at space axis. That is, the strength of the massive charge cannot change, according to the spatial environment. This is because the massive charge can be defined as the mixture (cancellation) of the right- and left-handed angular momentum elements at the

space axis (at $k_{p,total} = (+k_p) + (-k_p) = 0$) (i.e., $\langle R_R(+k_p) | H_{1,+k_p,-k_p} | R_L(-k_p) \rangle$ and $\langle L_L(+k_p) | H_{1,+k_p,-k_p} | L_R(-k_p) \rangle$). That is, we can consider that the massive charges are rigid with respect to the spatial environment. We can consider that the massive charge observed in our real world can be defined as the mixture (cancellation) of the components of angular momentum wave function for the right- (left-) handed particle and the right- (left-) handed antiparticle at space axis (at $k_{p,total} = (+k_p) + (-k_p) = 0$), as shown in Figs. 2 and 4.

5.3 Electric Monopole Charge

The energy $\varepsilon_{q_e,R}(q_e)$ for the right-handed chirality $|R \uparrow(q_e, +t_p)\rangle$ element can be defined as Eq. (37). At the time of the Big Bang, the $\varepsilon_{q_e,R}(q_e)$ value was the minimum ($c_{R_R}(q_e) = 1$). That is, there was no mixture between the right- $|R_R(+t_p)\rangle$ and left- $|R_L(-t_p)\rangle (= |R_L(+t_a)\rangle)$ handed helicity elements, and thus the electric monopole field energy was zero at the Big Bang. In other words, the electric monopole charge was not generated at that time (Fig. 14). However, after that, temperature significantly decreased, and thus because of any origin (i.e., Higgs boson, broken symmetry of chirality etc.), the mixture between the right- $|R_R(+t_p)\rangle$ and left- $|R_L(-t_p)\rangle (= |R_L(+t_a)\rangle)$ helicity elements at the time axis has begun to occur. The mixture between the right- $|R_R(+t_p)\rangle$ and left- $|R_L(-t_p)\rangle$ handed helicity elements at the time axis increases with an increase in time (with a decrease in the $c_{R_R}(q_e)$ value). Similar discussions can be made in the $|L \downarrow(q_e, +t_p)\rangle$ state.

The electric monopole field energy is proportional to the $\langle R_R(+t_p) | H_{0,+t_p} | R_R(+t_p) \rangle$ and $\langle L_L(+t_p) | H_{0,+t_p} | L_L(+t_p) \rangle$ values (Figs. 3 and 5). On the other hand, these values are different between the kinds of particles.

We can see from Figs. 3 and 5 that the $\varepsilon_{q_e,R}(q_e)$ and $\varepsilon_{q_e,L}(q_e)$ values are equivalent in the space axis. The total momentum in $\langle R_R(+t_p) | H_{0,+t_p} | R_R(+t_p) \rangle$ and

$\langle L_L(+t_p)H_{0,+t_p}|L_L(+t_p)\rangle$ terms in both $|R\uparrow(q_e,+t_p)\rangle$ and $|L\downarrow(q_e,+t_p)\rangle$ states are not zero. And the total chirality in the $\langle R_R(+t_p)H_{0,+t_p}|R_R(+t_p)\rangle$ and $\langle L_L(+t_p)H_{0,+t_p}|L_L(+t_p)\rangle$ terms in the $|R\uparrow(q_e,+t_p)\rangle$ and $|L\downarrow(q_e,+t_p)\rangle$ states are opposite by each other at time axis, as shown in Figs. 3 and 5. We can consider that the electric monopole charge is generated by the mixture of the right- $|R_R(+t_p)\rangle$ and left- $|R_L(-t_p)\rangle$ handed helicity elements at the time axis. For example, we can consider that the electric monopole charge is generated by the mixture (superposition) of the particle ($|R_R(+t_p)\rangle$) and antiparticle ($|R_L(-t_p)\rangle$) states components in the wavefunction in the particle ($|R\uparrow(q_e,+t_p)\rangle$). In the real world we live, the reversible process ($-t_p$) cannot be made in the time axis (irreversible). Therefore, we must consider the $\langle R_R(+t_p)H_{0,+t_p}|R_R(+t_p)\rangle$ and $\langle L_L(+t_p)H_{0,+t_p}|L_L(+t_p)\rangle$ states instead of the $\langle R_R(+t_p)H_{1,+t_p,-t_p}|R_L(-t_p)\rangle$ and $\langle L_L(+t_p)H_{1,+t_p,-t_p}|L_R(-t_p)\rangle$ states. This is the reason why the total chirality in the $\langle R_R(+t_p)H_{0,+t_p}|R_R(+t_p)\rangle$ and $\langle L_L(+t_p)H_{0,+t_p}|L_L(+t_p)\rangle$ values in the both $|R\uparrow(q_e,+t_p)\rangle$ and $|L\downarrow(q_e,+t_p)\rangle$ states are not zero, and opposite by each other, and the number of elements for electric monopole charge is two, and thus there are attractive and repulsive forces between two electric monopole charges. Because of the $\langle R_R(+t_p)H_{0,+t_p}|R_R(+t_p)\rangle$ terms, the electric monopole field only springs out from the infinitesimal source point to any direction in the space and time axes. On the other hand, because of the $\langle L_L(+t_p)H_{0,+t_p}|L_L(+t_p)\rangle$ terms, the electric field only comes into the infinitesimal sink point from any direction in the space and time axes. In summary, because of the $\langle R_R(+t_p)H_{1,+t_p,-t_p}|R_L(-t_p)\rangle$ and $\langle L_L(+t_p)H_{1,+t_p,-t_p}|L_R(-t_p)\rangle$ terms, originating from the mixture of the right- and left-handed helicity

elements, the electric field springs out from the infinitesimal source point to any direction in the time axis, or comes into the infinitesimal sink point from any direction in the time axis.

It should be noted that the strength of the electric monopole charge is observed to be always constant at time axis, and not to depend on the direction at space axis. That is, the strength of the electric monopole charge cannot change, according to the spatial and time environment. This is because the electric monopole charge can be defined as the mixture (cancellation) of the right- and left-handed angular momentum elements at the time axis (at $t_{p,total} = (+t_p) + (-t_p) = 0$) (i.e.,

$$\langle R_R(+t_p)H_{1,+t_p,-t_p}|R_L(-t_p)\rangle \quad \text{and} \\ \langle L_L(+t_p)H_{1,+t_p,-t_p}|L_R(-t_p)\rangle).$$

That is, we can consider that the electric monopole charges are rigid with respect to the spatial and time environment. We can consider that the electric monopole charge observed in our real world can be defined as the mixture (cancellation) of the components of angular momentum wave function for the right- (left-) handed particle and the right- (left-) handed antiparticle at the time axis, as shown in Figs. 3 and 5. The electric monopole charges are generated by the interactions between the wave functional components of the particles and antiparticles. We can interpret that the electric monopole charges are generated by the virtual particle-antiparticle pair annihilation interaction in a particle (at $k_{p,total} = (+k_p) + (+k_a) = 0$, at $t_{p,total} = (+t_p) + (+t_a) = 0$).

5.4 Color Charge

The $\varepsilon_{q_c,R}(q_e)$ for the right-handed chirality $|R\uparrow(q_e,+t_p)\rangle$ element can be defined as Eq. (36). At the time of the Big Bang, the $\varepsilon_{q_c,R}(q_e)$ value was very large ($c_{R_R}(q_e) = 1$). That is, there was no mixture between the right- $|R_R(+t_p)\rangle$ and left- $|R_L(-t_p)\rangle (= |R_L(+t_a)\rangle)$ handed helicity elements, and thus the color charge field was very large at the Big Bang (Fig. 14). However, after that, temperature significantly decreased, and thus because of any origin (Higgs boson, broken symmetry of chirality etc.), the mixture between the right- $|R_R(+t_p)\rangle$ and left- $|R_L(-t_p)\rangle (= |R_L(+t_a)\rangle)$ handed helicity elements at the time axis has begun to occur. The mixture between the right- $|R_R(+t_p)\rangle$ and

left- $\left| R_L(-t_p) \right\rangle$ handed helicity elements at the time axis increases with an increase in time (with decrease in the $c_{R_R}(q_e)$ value). The $\varepsilon_{q_c, R}(q_e)$ value decreases with an increase in time (with decrease in the $c_{R_R}(q_e)$ value). Similar discussions can be made in the $\left| L \downarrow (q_e, +t_p) \right\rangle$ state.

We can consider that the three kinds of the color charges (red (Rd), blue (Bl), and green (Gr)) states are composed from the three magnetic $\psi_{q_c, RL}(q_e)$, $\psi_{q_c, R}(q_e)$, and $\psi_{q_c, L}(q_e)$ states, having the energies of the $\varepsilon_{q_c, RL}(q_e)$ ($= \varepsilon_{q_m, R}(q_g)$ and $\varepsilon_{q_m, L}(q_g)$), $\varepsilon_{q_c, R}(q_e)$, and $\varepsilon_{q_c, L}(q_e)$, respectively. Red, blue, and green color charges can be defined by appropriate combination between $\psi_{q_c, RL}(q_e)$, $\psi_{q_c, R}(q_e)$, and $\psi_{q_c, L}(q_e)$ states. For example, we can consider that the energy for the color field originating from the red, blue, and green charges can be mainly expressed as the $\varepsilon_{q_c, R}(q_e)$, $\varepsilon_{q_c, L}(q_e)$, and $\varepsilon_{q_c, RL}(q_e)$ values, respectively. This consideration is available, at least, as essential qualitative discussions in this article. Three color charges (red, blue, and green) can be explained if we define the magnetic monopole and magnetic dipole moment expressed in Eqs. (13), (23), (36), and (45) as color charges. Therefore, we can consider that the color charges in the strong force can originate from the magnetic monopole and the spin magnetic dipole moment.

For example, wavefunction of the three quarks (Ψ_1 , Ψ_2 , and Ψ_3) in a proton or neutron can be expressed as

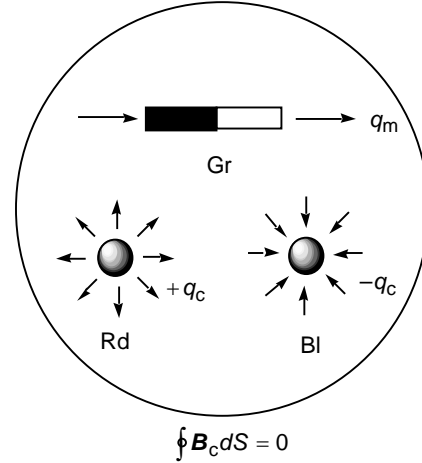
$$\Psi_1 = \sqrt{c_{1,int.}^2(q_e) + c_{1,ext.}^2(q_e)} \times \left\{ c_{R_R}(q_e) \Psi_{q_c, R} + c_{R_L}(q_e) \Psi_{q_c, L} \right\} \quad (101)$$

$$\Psi_2 = \sqrt{c_{2,int.}^2(q_e) + c_{2,ext.}^2(q_e)} \times \left\{ c_{L_L}(q_e) \Psi_{q_c, L} + c_{L_R}(q_e) \Psi_{q_c, R} \right\} \quad (102)$$

$$\Psi_3 = \sqrt{c_{3,int.}^2(q_e) + c_{3,ext.}^2(q_e)} c_{RL}(q_e) \Psi_{q_c, RL}, \quad (103)$$

$$(c_{1,int.}^2(q_e) + c_{1,ext.}^2(q_e)) (c_{R_R}^2(q_e) + c_{R_L}^2(q_e)) = 1, \quad (104)$$

$$(c_{2,int.}^2(q_e) + c_{2,ext.}^2(q_e)) (c_{L_L}^2(q_e) + c_{L_R}^2(q_e)) = 1, \quad (105)$$



Gauss's law in color field

Fig. 15. Gauss's law in the color field in a hadron and an anti-hadron.

$$(c_{3,int.}^2(q_e) + c_{3,ext.}^2(q_e)) c_{RL}^2(q_e) = 1, \quad (106)$$

where the $c_{1,int.}(q_e)$, $c_{2,int.}(q_e)$, and $c_{3,int.}(q_e)$ values are the internal coefficients denoting the strong field energy, and the $c_{1,ext.}(q_e)$, $c_{2,ext.}(q_e)$, and $c_{3,ext.}(q_e)$ values are the external coefficients denoting the color charges in quarks, antiquarks, and gluons. The space integration of the color charge field becomes zero in a hadron (Gauss's law in color charge) (Fig. 15),

$$\oint B_c dS = 0. \quad (107)$$

This is the reason why the total color charge in a hadron is observed to be 0 (white color charge), and the reason why gluons are observed to be confined within a hadron,

$$c_{1,ext.}^2(q_e) c_{R_R}^2(q_e) + c_{2,ext.}^2(q_e) c_{L_R}^2(q_e) = c_{1,ext.}^2(q_e) c_{R_L}^2(q_e) + c_{2,ext.}^2(q_e) c_{L_L}^2(q_e) \quad (108)$$

We can see from Figs. 3 and 5 that the $\varepsilon_{q_c, R}(q_e)$ and $\varepsilon_{q_c, L}(q_e)$ values are equivalent in the space axis. The total momentum in the $\left\langle R_R(+t_p) \right| H_{0,+t_p,+t_p} \left| R_R(+t_p) \right\rangle$ and $\left\langle L_L(+t_p) \right| H_{0,+t_p,+t_p} \left| L_L(+t_p) \right\rangle$ terms in the both $\left| R \uparrow (q_e, +t_p) \right\rangle$ and $\left| L \downarrow (q_e, +t_p) \right\rangle$ states are not zero. And the total chirality in the $\left\langle R_R(+t_p) \right| H_{0,+t_p,+t_p} \left| R_R(+t_p) \right\rangle$ and $\left\langle L_L(+t_p) \right| H_{0,+t_p,+t_p} \left| L_L(+t_p) \right\rangle$ terms in the

$\left| R \uparrow (q_e, +t_p) \right\rangle$ and $\left| L \downarrow (q_e, +t_p) \right\rangle$ states are opposite by each other at the time axis, as shown in Figs. 3 and 5. We can consider that the color charge is the right- $\left| R_R(+t_p) \right\rangle$ and left- $\left| R_L(-t_p) \right\rangle$ handed helicity elements of the angular momentum in quark at the time axis. In the real world we live, the reversible process ($-t_p$) cannot be possible in the time axis (irreversible). Therefore, we must consider the $-\left\langle R_R(+t_p) \right| H_{0,+t_p,+t_p} \left| R_R(+t_p) \right\rangle$ and $-\left\langle L_L(+t_p) \right| H_{0,+t_p,+t_p} \left| L_L(+t_p) \right\rangle$ states instead of the $\left\langle R_L(-t_p) \right| H_{0,+t_p,+t_p} \left| R_L(-t_p) \right\rangle$ and $\left\langle L_R(-t_p) \right| H_{0,+t_p,+t_p} \left| L_R(-t_p) \right\rangle$ states. This is the reason why the total chirality in the $\left\langle R_R(+t_p) \right| H_{0,+t_p,+t_p} \left| R_R(+t_p) \right\rangle$ and $\left\langle L_L(+t_p) \right| H_{0,+t_p,+t_p} \left| L_L(+t_p) \right\rangle$ values in the $\left| R \uparrow (q_e, +t_p) \right\rangle$ and $\left| L \downarrow (q_e, +t_p) \right\rangle$ states are not zero, and opposite by each other, and the number of elements for color charge at time axis is two. On the other hand, the number of elements for color charge at space axis is one. Furthermore, there is only attractive forces between two or three color charges. Because of the $\left\langle R_R(+t_p) \right| H_{0,+t_p,+t_p} \left| R_R(+t_p) \right\rangle$ terms, the color field only springs out from the infinitesimal source point to any direction in space and time axes. On the other hand, because of the $\left\langle L_L(+t_p) \right| H_{0,+t_p,+t_p} \left| L_L(+t_p) \right\rangle$ terms, the color field only comes into the infinitesimal sink point from any direction in space and time axes. In summary, because of the $\left\langle R_R(+t_p) \right| H_{0,+t_p,+t_p} \left| R_R(+t_p) \right\rangle$ and $\left\langle L_L(+t_p) \right| H_{0,+t_p,+t_p} \left| L_L(+t_p) \right\rangle$ terms, originating from the right- $\left| R_R(+t_p) \right\rangle$ and left- $\left| R_L(-t_p) \right\rangle$ handed helicity elements, and the left- $\left| L_L(+t_p) \right\rangle$ and right- $\left| L_R(-t_p) \right\rangle$ handed helicity elements, of the angular momentum in quark at the time axis, the color field springs out from the infinitesimal source point to any direction in time axis, or comes into the infinitesimal sink point from any direction in the time axis.

It should be noted that the strength of the color charge depends on time and the direction at the space axis. That is, the strength of the color charge can change, according to the time change and the spatial environment. This is because the color charge can be defined as the summation

between the right- $\left\langle R_R(+t_p) \right| H_{0,+t_p,+t_p} \left| R_R(+t_p) \right\rangle$ and left-handed $\left\langle R_L(-t_p) \right| H_{0,+t_p,+t_p} \left| R_L(-t_p) \right\rangle$ angular elements, and the left- $\left\langle L_L(+t_p) \right| H_{0,+t_p,+t_p} \left| L_L(+t_p) \right\rangle$ and right-handed $\left\langle L_R(-t_p) \right| H_{0,+t_p,+t_p} \left| L_R(-t_p) \right\rangle$ angular elements (time $t_p (\neq 0)$ dependent ($+t_p$ or $-t_p$)). That is, we can consider that the color charges are not rigid with respect to time change and the spatial environment. We can consider that the color charge observed in our real world can be defined as the summation of the angular momentum of the components of wave function for the right- (left-) handed particle and the right- (left-) handed antiparticle at particle time axis, as shown in Figs. 3 and 5. That is, we can consider that total color charges for hadrons are always 0 (while) because each color charge for quarks and antiquarks can change with time so that the total external energy for the environments for hadrons can be minimum and stable (total while color charge). There is a possibility that even if each quarks and antiquarks could be separated, each quark or antiquark has zero color charge (i.e., green charge defined in this article), and thus we would not be able to observe the strong color charges (i.e., red and blue charges defined in this article). There is a possibility that the color charges for leptons and antileptons, which can be observed to be isolated, cannot be observed even if leptons and antileptons as well as the quarks and antiquarks have color charges.

If we observe the color charge for long enough time ($\Delta t \gg 0$), we would observe average $\varepsilon_{q_c, R, obs. \Delta t \gg 0}$ and $\varepsilon_{q_c, L, obs. \Delta t \gg 0}$ values originating from the both the $\left\langle R_R(+t_p) \right| H_{0,+t_p,+t_p} \left| R_R(+t_p) \right\rangle$ and $\left\langle R_L(-t_p) \right| H_{0,+t_p,+t_p} \left| R_L(-t_p) \right\rangle$ terms, and from the both the $\left\langle L_L(+t_p) \right| H_{0,+t_p,+t_p} \left| L_L(+t_p) \right\rangle$ and $\left\langle L_R(-t_p) \right| H_{0,+t_p,+t_p} \left| L_R(-t_p) \right\rangle$ terms,

$$\varepsilon_{q_c, R, obs. \Delta t \gg 0} = (2c_{R_R}^2 (q_e) - 1) \varepsilon_{q_{\infty}, R}, \quad (109)$$

$$\varepsilon_{q_c, L, obs. \Delta t \gg 0} = (2c_{L_L}^2 (q_e) - 1) \varepsilon_{q_{\infty}, L}. \quad (110)$$

On the other hand, if we observe the color charge for short enough time ($\Delta t \approx 0$), we would observe various $\varepsilon_{q_c, R, obs. \Delta t \approx 0}$ and $\varepsilon_{q_c, L, obs. \Delta t \approx 0}$ values originating from only the $\left\langle R_R(+t_p) \right| H_{0,+t_p,+t_p} \left| R_R(+t_p) \right\rangle$, or

$\langle R_L(-t_p)H_{0,+t_p,+t_p} | R_L(-t_p) \rangle$, or other combinations between them, and from only the $\langle L_L(+t_p)H_{0,+t_p,+t_p} | L_L(+t_p) \rangle$, or $\langle L_R(-t_p)H_{0,+t_p,+t_p} | L_R(-t_p) \rangle$, or other combinations between them,

$$\begin{aligned} \varepsilon_{q_c, R, \text{obs. } \Delta t \approx 0} &= \varepsilon_{q_{c\infty}, R} \\ &= \varepsilon_{q_{c\infty}, L} \\ &= \text{etc.} \end{aligned} \quad (111)$$

$$\begin{aligned} \varepsilon_{q_c, L, \text{obs. } \Delta t \approx 0} &= \varepsilon_{q_{c\infty}, L} \\ &= \varepsilon_{q_{c\infty}, R} \\ &= \text{etc.} \end{aligned} \quad (112)$$

That is, if we observe the color charge for long enough time (i.e., the uncertainty of the time is very large ($\Delta t \gg 0$)), we would observe the average $\varepsilon_{q_c, R, \text{obs. } \Delta t \gg 0}$ and $\varepsilon_{q_c, L, \text{obs. } \Delta t \gg 0}$ values with very small uncertainty in energy ($\Delta E \approx 0$). On the other hand, if we observe the color charge in small enough time (i.e., the uncertainty of the time is very short ($\Delta t \approx 0$)), we would observe the various $\varepsilon_{q_c, R, \text{obs. } \Delta t \approx 0}$ and $\varepsilon_{q_c, L, \text{obs. } \Delta t \approx 0}$ values with very large uncertainty in energy ($\Delta E \gg 0$). This can be related to the Heisenberg's uncertainty principle. This is the reason why the gluon has the color charge energies ($\varepsilon_{q_c, R, \text{ext.}}(q_e)$) as well as the strong force field energies ($\varepsilon_{q_c, R, \text{int.}}(q_e)$), and the reason why the color charges and the number of gluons significantly change in a hadron with a time change.

6. Relationships between the Spin Magnetic Dipole Moment, Massive Charge, Electric Monopole Charge, and Color Charge; Antiparticles at the Particle Time Axis

Various charges for antiparticles should be expressed at the antiparticle spacetime axis. On the other hand, these charges will be expressed at the particle spacetime axis where we live as a real world, in this article. That is, anti-red, anti-blue, and anti-green color charges at the antiparticle spacetime axis are denoted as blue, red, and green color charges at the particle spacetime axis. Anti-positive and anti-negative electric charges at the antiparticle spacetime axis are denoted as negative and positive electric charges at the particle spacetime axis. Furthermore, anti-N and anti-S magnetic poles at the antiparticle spacetime axis are denoted as S and N magnetic poles at the particle spacetime axis.

6.1 Spin Magnetic Dipole Moment

The energies for the spin magnetic dipole moment for the $|R \uparrow(q_g, -k_p)\rangle$ state can be expressed as Eq. (61). At the time of the Big Bang, the $\varepsilon_{q_m, R}(q_g)$ and $\varepsilon_{q_m, L}(q_g)$ values were the maximum. That is, there was no mixture between the right- $|R_R(-k_p)\rangle$ and left- $|R_L(+k_p)\rangle (= |R_L(-k_a)\rangle)$ handed helicity elements, and thus the spin magnetic dipole moment was the largest at the Big Bang. In other words, the mass (infinitesimal electric dipole charge) and electric monopole charge were not generated at that time (Fig. 14). However, since temperatures immediately decreased after Big Bang, because of any origin (i.e., Higgs boson, broken symmetry of chirality etc.), the mixture between the right- $|R_R(-k_p)\rangle$ and left- $|R_L(+k_p)\rangle$ handed helicity elements has begun to occur. The mixture between the right- $|R_R(-k_p)\rangle$ and left- $|R_L(+k_p)\rangle$ handed helicity elements increases with an increase in time (with a decrease in the $c_{R_R}(q_g)$ value). Similar discussions can be made in the $|L \downarrow(q_g, -k_p)\rangle$ state.

We can see from Figs. 10 and 12 that the $\varepsilon_{q_m, R}(q_g)$ and $\varepsilon_{q_m, L}(q_g)$ values are not equivalent in the space axis. The total chirality and momentum in the $\langle R_R(-k_p)H_{0,-k_p,-k_p} | R_R(-k_p) \rangle$ and $\langle L_L(-k_p)H_{0,-k_p,-k_p} | L_L(-k_p) \rangle$ terms in the both $|R \uparrow(q_g, -k_p)\rangle$ and $|L \downarrow(q_g, -k_p)\rangle$ states are not zero. This is the reason why the number of elements for magnetic spin dipole moments is two, and thus there are attractive and repulsive forces between two magnetic dipole moments.

The spin magnetic dipole energy is proportional to the $\langle R_R(-k_p)H_{0,-k_p,-k_p} | R_R(-k_p) \rangle$ and $\langle R_L(+k_p)H_{0,-k_p,-k_p} | R_L(+k_p) \rangle$ values, and the $\langle L_L(-k_p)H_{0,-k_p,-k_p} | L_L(-k_p) \rangle$ and $\langle L_R(+k_p)H_{0,-k_p,-k_p} | L_R(+k_p) \rangle$ values (Figs. 10 and 12). These values are different between the kinds of particles and antiparticles. This is the reason why we cannot theoretically predict the intensity of the spin

magnetic dipole moment for each particle or antiparticle. In summary, because of the $\langle \mathbf{R}_R(-k_p) | H_{0,-k_p,-k_p} | \mathbf{R}_R(-k_p) \rangle$ and $\langle \mathbf{L}_L(-k_p) | H_{0,-k_p,-k_p} | \mathbf{L}_L(-k_p) \rangle$ terms, originating from the finite right- and left-handed helicity elements, respectively, the magnetic dipole field goes from the infinitesimal source point to infinitesimal sink point at finite space axis. This is the reason why the path of the magnetic dipole field is like loop (source-sink)-type, as shown in Figs. 10 and 12.

It should be noted that the strength of the spin magnetic dipole moment depends on the direction at the space axis. That is, the strength of the spin magnetic dipole moment can change, according to the spatial environment. This is because the spin magnetic dipole moment can be defined as the difference between the right- $\langle \mathbf{R}_R(-k_p) | H_{0,-k_p,-k_p} | \mathbf{R}_R(-k_p) \rangle$ and left-handed $\langle \mathbf{R}_L(+k_p) | H_{0,-k_p,-k_p} | \mathbf{R}_L(+k_p) \rangle$ angular momentum elements (space $k_p (\neq 0)$ dependent ($+k_p$ or $-k_p$)). That is, we can consider that the spin magnetic dipole moments are not rigid with respect to the spatial environment. We can consider that the spin magnetic dipole moment observed in our real world can be defined as the difference of the spin angular momentum between the components of wave function for the right- (left-) handed particle and the right- (left-) handed antiparticle, as shown in Figs. 10 and 12.

If we observe the magnetic dipole moment in large enough range and time ($\Delta r \gg 0, t \gg 0$), we would observe average $\varepsilon_{q_m, \mathbf{R}, \text{obs. } \Delta r, t \gg 0}$ and $\varepsilon_{q_m, \mathbf{L}, \text{obs. } \Delta r, t \gg 0}$ values originating from both the $\langle \mathbf{R}_R(-k_p) | H_{0,-k_p,-k_p} | \mathbf{R}_R(-k_p) \rangle$ and $\langle \mathbf{R}_L(+k_p) | H_{0,-k_p,-k_p} | \mathbf{R}_L(+k_p) \rangle$ terms, and both the $\langle \mathbf{L}_L(-k_p) | H_{0,-k_p,-k_p} | \mathbf{L}_L(-k_p) \rangle$ and $\langle \mathbf{L}_R(+k_p) | H_{0,-k_p,-k_p} | \mathbf{L}_R(+k_p) \rangle$ terms, respectively,

$$\varepsilon_{q_m, \mathbf{R}, \text{obs. } \Delta r, t \gg 0} = (2c_{\mathbf{R}_R}^2(q_g) - 1) \varepsilon_{q_{m\infty}, \mathbf{R}} \quad (113)$$

$$\varepsilon_{q_m, \mathbf{L}, \text{obs. } \Delta r, t \gg 0} = (2c_{\mathbf{L}_L}^2(q_g) - 1) \varepsilon_{q_{m\infty}, \mathbf{L}} \quad (114)$$

On the other hand, if we observe the magnetic dipole moment in small enough range and time ($\Delta r \approx 0, \Delta t \approx 0$), we would observe various $\varepsilon_{q_m, \mathbf{R}, \text{obs. } \Delta r, t \approx 0}$ and

$\varepsilon_{q_m, \mathbf{L}, \text{obs. } \Delta r, t \approx 0}$ values originating from only the $\langle \mathbf{R}_R(-k_p) | H_{0,-k_p,-k_p} | \mathbf{R}_R(-k_p) \rangle$, or $\langle \mathbf{R}_L(+k_p) | H_{0,-k_p,-k_p} | \mathbf{R}_L(+k_p) \rangle$, or other combinations between them, and from only the $\langle \mathbf{L}_L(-k_p) | H_{0,-k_p,-k_p} | \mathbf{L}_L(-k_p) \rangle$, or $\langle \mathbf{L}_R(+k_p) | H_{0,-k_p,-k_p} | \mathbf{L}_R(+k_p) \rangle$, or other combinations between them,

$$\begin{aligned} \varepsilon_{q_m, \mathbf{R}, \text{obs. } \Delta r, t \approx 0} &= \varepsilon_{q_{m\infty}, \mathbf{R}} \\ &= \varepsilon_{q_{m\infty}, \mathbf{L}} \\ &= \text{etc.} \end{aligned} \quad (115)$$

$$\begin{aligned} \varepsilon_{q_m, \mathbf{L}, \text{obs. } \Delta r \approx 0} &= \varepsilon_{q_{m\infty}, \mathbf{L}} \\ &= \varepsilon_{q_{m\infty}, \mathbf{R}} \\ &= \text{etc.} \end{aligned} \quad (116)$$

That is, if we observe the magnetic dipole moment in large enough range and time (i.e., the uncertainty of the position and time is very large ($\Delta r \gg 0, t \gg 0$), we would observe the average $\varepsilon_{q_m, \mathbf{R}, \text{obs. } \Delta r, t \gg 0}$ and $\varepsilon_{q_m, \mathbf{L}, \text{obs. } \Delta r, t \gg 0}$ values with very small uncertainty in momentum and energy ($\Delta k \approx 0, \Delta E \approx 0$), as usual. On the other hand, if we observe the magnetic dipole moment in small enough range and time (i.e., the uncertainty of the position and time is very small ($\Delta r \approx 0, \Delta t \approx 0$), we would observe the various $\varepsilon_{q_m, \mathbf{R}, \text{obs. } \Delta r, t \approx 0}$ and $\varepsilon_{q_m, \mathbf{L}, \text{obs. } \Delta r, t \approx 0}$ values with very large uncertainty in momentum and energy ($\Delta k \gg 0, \Delta E \gg 0$). This can be related to the Heisenberg's uncertainty principle.

6.2 Mass (Infinitesimal Electric (and Magnetic) Dipole Charge)

The mass energy $\varepsilon_{q_g, \mathbf{R}}(q_g)$ for the right-handed chirality $|\mathbf{R} \uparrow(q_g, -k_p)\rangle$ element can be defined as Eq. (58). At the time of the Big Bang, the $\varepsilon_{q_g, \mathbf{R}}(q_g)$ value was the minimum ($c_{\mathbf{R}_R}(q_g) = 1$). That is, there was no mixture between the right- $|\mathbf{R}_R(-k_p)\rangle$ and left- $|\mathbf{R}_L(+k_p)\rangle$ handed helicity elements, and thus the mass energy was zero at the Big Bang. In other words, the mass was not generated at that time (Fig. 14). However, after that, temperature significantly decreased, and thus because of any origin (i.e., Higgs boson, broken symmetry of chirality etc.), the mixture between the right-

$\left| R_R(-k_p) \right\rangle$ and left- $\left| R_L(+k_p) \right\rangle$ handed helicity elements has begun to occur. The mixture between the right- $\left| R_R(-k_p) \right\rangle$ and left- $\left| R_L(+k_p) \right\rangle$ handed helicity elements increases with an increase in time (with a decrease in the $c_{R_R}(q_g)$ value). Similar discussions can be made in the $\left| L \downarrow (q_g, -k_p) \right\rangle$ state.

The mass energy is proportional to the $\left\langle R_R(-k_p) \middle| H_{1,-k_p,+k_p} \middle| R_L(+k_p) \right\rangle$ and $\left\langle L_L(-k_p) \middle| H_{1,-k_p,+k_p} \middle| L_R(+k_p) \right\rangle$ values (Figs. 10 and 12).

These values are different between the kinds of particles. This is the reason why we do not theoretically predict the mass for each particle or antiparticle.

We can see from Figs. 10 and 12 that the $\varepsilon_{q_g,R}(q_g)$ and $\varepsilon_{q_g,L}(q_g)$ values are equivalent in the space axis. The total chirality and momentum in the $\left\langle R_R(-k_p) \middle| H_{1,-k_p,+k_p} \middle| R_L(+k_p) \right\rangle$ and $\left\langle L_L(-k_p) \middle| H_{1,-k_p,+k_p} \middle| L_R(+k_p) \right\rangle$ terms in the both $\left| R \uparrow (q_g, -k_p) \right\rangle$ and $\left| L \downarrow (q_g, -k_p) \right\rangle$ states are zero. We can consider that the mass is generated by the mixture of the right- $\left| R_R(-k_p) \right\rangle$ and left- $\left| R_L(+k_p) \right\rangle$ handed helicity elements at the space axis. In the real world we live, the reversible process ($-k_p$) can be possible in the space axis while the reversible process ($-t_p$) cannot be possible in the time axis (irreversible). This is the reason why the number of elements for mass is only one, and thus there is only attractive force between two masses.

In summary, because of the $\left\langle R_R(-k_p) \middle| H_{1,-k_p,+k_p} \middle| R_L(+k_p) \right\rangle$ and $\left\langle L_L(-k_p) \middle| H_{1,-k_p,+k_p} \middle| L_R(+k_p) \right\rangle$ terms, originating from the cancellation of the right- and left-handed helicity elements at space axis, the gravitational fields only spring out from the infinitesimal source point (or comes into the infinitesimal sink point) to (from) any direction in the space axis.

On the other hand, the total chirality and momentum in the $\left\langle R_R(-k_p) \middle| H_{1,-k_p,+k_p} \middle| R_L(+k_p) \right\rangle$ and $\left\langle L_L(-k_p) \middle| H_{1,-k_p,+k_p} \middle| L_R(+k_p) \right\rangle$ states are zero not because of the intrinsic zero value but because of the cancellation of the large right- and left-handed helicity elements, which are the origin of the spin magnetic

moment and the electric charge. Therefore, there is a possibility that the external potential energy ($\varepsilon_{q_g,\text{ext},R}(q_g)$ and $\varepsilon_{q_g,\text{ext},L}(q_g)$) for the $\left\langle R_R(-k_p) \middle| H_{1,-k_p,+k_p} \middle| R_L(+k_p) \right\rangle$ and $\left\langle L_L(-k_p) \middle| H_{1,-k_p,+k_p} \middle| L_R(+k_p) \right\rangle$ states can be very small but finite values (fluctuated and induced polarization effects). Therefore, the distortion of the spacetime axes can occur. That is, we can consider that the gravity can be considered to be the residual electromagnetic forces [14]. Such fluctuation originates from the fact that the q_g value is decided under the very small uncertainty of the position ($\Delta r \approx 0$) and time ($\Delta t \approx 0$), and thus the uncertainty of the momentum ($\Delta k \gg 0$) and energy ($\Delta E \gg 0$) is very large (Heisenberg's uncertainty principle).

Most of extremely large energy generated at the time of the Big Bang has been stored in the particle and antiparticle as a large potential rest energy, and only small part of it is now used as very small gravitational energy. This is the reason why the gravity is much smaller than other three forces.

It should be noted that the strength of the massive charge is observed to be always constant, and not to depend on the direction at space axis. That is, the strength of the massive charge cannot change, according to the spatial environment. This is because the massive charge can be defined as the mixture (cancellation) of the right- and left-handed angular momentum elements at the space axis (at $k_{p,\text{total}} = (+k_p) + (-k_p) = 0$) (i.e., $\left\langle R_R(-k_p) \middle| H_{1,-k_p,+k_p} \middle| R_L(+k_p) \right\rangle$ and $\left\langle L_L(-k_p) \middle| H_{1,-k_p,+k_p} \middle| L_R(+k_p) \right\rangle$). That is, we can consider that the massive charges are rigid with respect to the spatial environment. We can consider that the massive charge observed in our real world can be defined as the mixture (cancellation) of the components of angular momentum wave function for the right- (left-) handed particle and the right- (left-) handed antiparticle at space axis (at $k_{p,\text{total}} = (+k_p) + (-k_p) = 0$), as shown in Figs. 10 and 12.

6.3 Electric Monopole Charge

The energy $\varepsilon_{q_e,R}(q_e)$ for the right-handed chirality $\left| R \uparrow (q_e, -t_p) \right\rangle$ element can be defined as Eq. (85). At the time of the Big Bang, the $\varepsilon_{q_e,R}(q_e)$ value was the minimum ($c_{R_R}(q_e) = 1$). That is, there was no mixture

between the right- $\left| \mathbf{R}_R(-t_p) \right\rangle$ and left- $\left| \mathbf{R}_L(+t_p) \right\rangle (= \left| \mathbf{R}_L(-t_a) \right\rangle)$ handed helicity elements, and thus the electric monopole field energy was zero at the Big Bang. In other words, the electric monopole charge was not generated at that time (Fig. 14). However, after that, temperature significantly decreased, and thus because of any origin (i.e., Higgs boson, broken symmetry of chirality etc.), the mixture between the right- $\left| \mathbf{R}_R(-t_p) \right\rangle$ and left- $\left| \mathbf{R}_L(+t_p) \right\rangle (= \left| \mathbf{R}_L(-t_a) \right\rangle)$ helicity elements at the time axis has begun to occur. The mixture between the right- $\left| \mathbf{R}_R(-t_p) \right\rangle$ and left- $\left| \mathbf{R}_L(+t_p) \right\rangle$ handed helicity elements at the time axis increases with an increase in time (with a decrease in the $c_{R_R}(q_e)$ value). Similar discussions can be made in the $\left| \mathbf{L} \downarrow(q_e, -t_p) \right\rangle$ state.

The electric monopole field energy is proportional to the $\left\langle \mathbf{R}_L(+t_p) \right| H_{0,+t_p} \left| \mathbf{R}_L(+t_p) \right\rangle$ and $\left\langle \mathbf{L}_R(+t_p) \right| H_{0,+t_p} \left| \mathbf{L}_R(+t_p) \right\rangle$ values (Figs. 11 and 13). On the other hand, these values are different between the kinds of particles.

We can see from Figs. 11 and 13 that the $\varepsilon_{q_e, R}(q_e)$ and $\varepsilon_{q_e, L}(q_e)$ values are equivalent in the space axis. The total momentum in $\left\langle \mathbf{R}_L(+t_p) \right| H_{0,+t_p} \left| \mathbf{R}_L(+t_p) \right\rangle$ and $\left\langle \mathbf{L}_R(+t_p) \right| H_{0,+t_p} \left| \mathbf{L}_R(+t_p) \right\rangle$ terms in both $\left| \mathbf{R} \uparrow(q_e, -t_p) \right\rangle$ and $\left| \mathbf{L} \downarrow(q_e, -t_p) \right\rangle$ states are not zero. And the total chirality in the $\left\langle \mathbf{R}_L(+t_p) \right| H_{0,+t_p} \left| \mathbf{R}_L(+t_p) \right\rangle$ and $\left\langle \mathbf{L}_R(+t_p) \right| H_{0,+t_p} \left| \mathbf{L}_R(+t_p) \right\rangle$ terms in the $\left| \mathbf{R} \uparrow(q_e, -t_p) \right\rangle$ and $\left| \mathbf{L} \downarrow(q_e, -t_p) \right\rangle$ states are opposite by each other at time axis, as shown in Figs. 11 and 13. We can consider that the electric monopole charge is generated by the mixture of the right- $\left| \mathbf{R}_R(-t_p) \right\rangle$ and left- $\left| \mathbf{R}_L(+t_p) \right\rangle$ handed helicity elements at the time axis. For example, we can consider that the electric monopole charge is generated by the mixture (superposition) of the antiparticle ($\left| \mathbf{R}_R(-t_p) \right\rangle$) and particle ($\left| \mathbf{R}_L(+t_p) \right\rangle$) states components in the wavefunction in the antiparticle ($\left| \mathbf{R} \uparrow(q_e, -t_p) \right\rangle$). In the real world we live, the reversible process ($-t_p$) cannot be made in the time axis

(irreversible). Therefore, we must consider the $\left\langle \mathbf{R}_L(+t_p) \right| H_{0,+t_p} \left| \mathbf{R}_L(+t_p) \right\rangle$ and $\left\langle \mathbf{L}_R(+t_p) \right| H_{0,+t_p} \left| \mathbf{L}_R(+t_p) \right\rangle$ states instead of the $\left\langle \mathbf{R}_R(-t_p) \right| H_{1,-t_p,+t_p} \left| \mathbf{R}_L(+t_p) \right\rangle$ and $\left\langle \mathbf{L}_L(-t_p) \right| H_{1,-t_p,+t_p} \left| \mathbf{L}_R(+t_p) \right\rangle$ states. This is the reason why the total chirality in the $\left\langle \mathbf{R}_L(+t_p) \right| H_{0,+t_p} \left| \mathbf{R}_L(+t_p) \right\rangle$ and $\left\langle \mathbf{L}_R(+t_p) \right| H_{0,+t_p} \left| \mathbf{L}_R(+t_p) \right\rangle$ values in the both $\left| \mathbf{R} \uparrow(q_e, -t_p) \right\rangle$ and $\left| \mathbf{L} \downarrow(q_e, -t_p) \right\rangle$ states are not zero, and opposite by each other, and the number of elements for electric monopole charge is two, and thus there are attractive and repulsive forces between two electric monopole charges. Because of the $\left\langle \mathbf{R}_L(+t_p) \right| H_{0,+t_p} \left| \mathbf{R}_L(+t_p) \right\rangle$ terms, the electric monopole field only springs out from the infinitesimal source point to any direction in the space and time axes. On the other hand, because of the $\left\langle \mathbf{L}_R(+t_p) \right| H_{0,+t_p} \left| \mathbf{L}_R(+t_p) \right\rangle$ terms, the electric field only comes into the infinitesimal sink point from any direction in the space and time axes. In summary, because of the $\left\langle \mathbf{R}_R(-t_p) \right| H_{1,-t_p,+t_p} \left| \mathbf{R}_L(+t_p) \right\rangle$ and $\left\langle \mathbf{L}_L(-t_p) \right| H_{1,-t_p,+t_p} \left| \mathbf{L}_R(+t_p) \right\rangle$ terms, originating from the mixture of the right- and left-handed helicity elements, the electric field springs out from the infinitesimal source point to any direction in the time axis, or comes into the infinitesimal sink point from any direction in the time axis.

It should be noted that the strength of the electric monopole charge is observed to be always constant at time axis, and not to depend on the direction at space axis. That is, the strength of the electric monopole charge cannot change, according to the spatial and time environment. This is because the electric monopole charge can be defined as the mixture (cancellation) of the right- and left-handed angular momentum elements at the time axis (at $t_{p,\text{total}} = (+t_p) + (-t_p) = 0$) (i.e., $\left\langle \mathbf{R}_R(-t_p) \right| H_{1,-t_p,+t_p} \left| \mathbf{R}_L(+t_p) \right\rangle$ and $\left\langle \mathbf{L}_L(-t_p) \right| H_{1,-t_p,+t_p} \left| \mathbf{L}_R(+t_p) \right\rangle$). That is, we can consider that the electric monopole charges are rigid with respect to the spatial and time environment. We can consider that the electric monopole charge observed in our real world can be defined as the mixture (cancellation) of the components of angular momentum wave function for the

right- (left-) handed particle and the right- (left-) handed antiparticle at the time axis, as shown in Fig. 1.

The electric monopole charges in antiparticles are generated by the interactions between the wave functional components of the antiparticles and particles. We can interpret that the electric monopole charges are generated by the virtual antiparticle-particle pair annihilation interaction in an antiparticle (at $k_{a,total} = (+k_a) + (+k_p) = 0$), at $t_{a,total} = (+t_a) + (+t_p) = 0$.

6.4 Color Charge

The $\varepsilon_{q_c, R}(q_e)$ for the right-handed chirality $\left| R \uparrow (q_e, -t_p) \right\rangle$ element can be defined as Eq. (84). At the time of the Big Bang, the $\varepsilon_{q_c, R}(q_e)$ value was very large ($c_{R_R}(q_e) = 1$). That is, there was no mixture between the right- $\left| R_R(-t_p) \right\rangle$ and left- $\left| R_L(+t_p) \right\rangle (= \left| R_L(-t_a) \right\rangle)$ handed helicity elements, and thus the color charge field was very large at the Big Bang (Fig. 14). However, after that, temperature significantly decreased, and thus because of any origin (Higgs boson, broken symmetry of chirality etc.), the mixture between the right- $\left| R_R(-t_p) \right\rangle$ and left- $\left| R_L(+t_p) \right\rangle (= \left| R_L(-t_a) \right\rangle)$ handed helicity elements at the time axis has begun to occur. The mixture between the right- $\left| R_R(-t_p) \right\rangle$ and left- $\left| R_L(+t_p) \right\rangle$ handed helicity elements at the time axis increases with an increase in time (with decrease in the $c_{R_R}(q_e)$ value). The $\varepsilon_{q_c, R}(q_e)$ value decreases with an increase in time (with decrease in the $c_{R_R}(q_e)$ value). Similar discussions can be made in the $\left| L \downarrow (q_e, -t_p) \right\rangle$ state.

We can consider that the three kinds of the color charges (red (Rd), blue (Bl), and green (Gr)) states are composed from the three magnetic $\psi_{q_c, RL}(q_e)$, $\psi_{q_c, R}(q_e)$, and $\psi_{q_c, L}(q_e)$ states, having the energies of the $\varepsilon_{q_c, RL}(q_e) (= \varepsilon_{q_m, R}(q_g) \text{ and } \varepsilon_{q_m, L}(q_g))$, $\varepsilon_{q_c, R}(q_e)$, and $\varepsilon_{q_c, L}(q_e)$, respectively. Red, blue, and green color charges can be defined by appropriate combination between $\psi_{q_c, RL}(q_e)$, $\psi_{q_c, R}(q_e)$, and $\psi_{q_c, L}(q_e)$ states. For example, we can consider that the energy for the color field originating from the red, blue, and green charges can be mainly expressed as the $\varepsilon_{q_c, R}(q_e)$, $\varepsilon_{q_c, L}(q_e)$, and

$\varepsilon_{q_c, RL}(q_e)$ values, respectively. This consideration is available, at least, as essential qualitative discussions in this article. Three color charges (red, blue, and green) can be explained if we define the magnetic monopole and magnetic dipole moment expressed in Eqs. (61), (71), (84), and (93) as color charges. Therefore, we can consider that the color charges in the strong force can originate from the magnetic monopole and the spin magnetic dipole moment.

For example, wavefunction of the three antiquarks (Ψ_1 , Ψ_2 , and Ψ_3) in an anti-proton or anti-neutron can be expressed as

$$\Psi_1 = \sqrt{c_{1,int.}^2(q_e) + c_{1,ext.}^2(q_e)} \times \left\{ c_{R_R}(q_e) \Psi_{q_c, R} + c_{R_L}(q_e) \Psi_{q_c, L} \right\} \quad (117)$$

$$\Psi_2 = \sqrt{c_{2,int.}^2(q_e) + c_{2,ext.}^2(q_e)} \times \left\{ c_{L_L}(q_e) \Psi_{q_c, L} + c_{L_R}(q_e) \Psi_{q_c, R} \right\} \quad (118)$$

$$\Psi_3 = \sqrt{c_{3,int.}^2(q_e) + c_{3,ext.}^2(q_e)} c_{RL}(q_e) \Psi_{q_c, RL}, \quad (119)$$

$$(c_{1,int.}^2(q_e) + c_{1,ext.}^2(q_e))(c_{R_R}^2(q_e) + c_{R_L}^2(q_e)) = 1, \quad (120)$$

$$(c_{2,int.}^2(q_e) + c_{2,ext.}^2(q_e))(c_{L_L}^2(q_e) + c_{L_R}^2(q_e)) = 1, \quad (121)$$

$$(c_{3,int.}^2(q_e) + c_{3,ext.}^2(q_e))c_{RL}^2(q_e) = 1, \quad (122)$$

where the $c_{1,int.}(q_e)$, $c_{2,int.}(q_e)$, and $c_{3,int.}(q_e)$ values are the internal coefficients denoting the strong field energy, and the $c_{1,ext.}(q_e)$, $c_{2,ext.}(q_e)$, and $c_{3,ext.}(q_e)$ values are the external coefficients denoting the color charges in quarks, antiquarks, and gluons. The space integration of the color charge field becomes zero in an anti-hadron (Gauss's law in color charge) (Fig. 15),

$$\oint B_c dS = 0. \quad (123)$$

This is the reason why the total color charge in an anti-hadron is observed to be 0 (white color charge), and the reason why gluons are observed to be confined within an anti-hadron.

$$c_{1,ext.}^2(q_e)c_{R_R}^2(q_e) + c_{2,ext.}^2(q_e)c_{L_R}^2(q_e)$$

$$= c_{1,ext.}^2(q_e)c_{R_L}^2(q_e) + c_{2,ext.}^2(q_e)c_{L_L}^2(q_e). \quad (124)$$

We can see from Figs. 11 and 13 that the $\varepsilon_{q_c,R}(q_e)$ and $\varepsilon_{q_c,L}(q_e)$ values are equivalent in the space axis. The total momentum in the $\langle R_L(+t_p)H_{0,-t_p,-t_p} | R_L(+t_p) \rangle$ and $\langle L_R(+t_p)H_{0,-t_p,-t_p} | L_R(+t_p) \rangle$ terms in the both $|R \uparrow(q_e,-t_p)\rangle$ and $|L \downarrow(q_e,-t_p)\rangle$ states are not zero. And the total chirality in the $\langle R_L(+t_p)H_{0,-t_p,-t_p} | R_L(+t_p) \rangle$ and $\langle L_R(+t_p)H_{0,-t_p,-t_p} | L_R(+t_p) \rangle$ terms in the $|R \uparrow(q_e,-t_p)\rangle$ and $|L \downarrow(q_e,-t_p)\rangle$ states are opposite by each other at the time axis, as shown in Figs. 11 and 13. We can consider that the color charge is the right- $|R_R(-t_p)\rangle$ and left- $|R_L(+t_p)\rangle$ handed helicity elements of the angular momentum in antiquark at the time axis. In the real world we live, the reversible process ($-t_p$) cannot be possible in the time axis (irreversible). Therefore, we must consider the $-\langle R_L(+t_p)H_{0,-t_p,-t_p} | R_L(+t_p) \rangle$ and $-\langle L_R(+t_p)H_{0,-t_p,-t_p} | L_R(+t_p) \rangle$ states instead of the $\langle R_R(-t_p)H_{0,-t_p,-t_p} | R_R(-t_p) \rangle$ and $\langle L_L(-t_p)H_{0,-t_p,-t_p} | L_L(-t_p) \rangle$ states. This is the reason why the total chirality in the $\langle R_L(+t_p)H_{0,-t_p,-t_p} | R_L(+t_p) \rangle$ and $\langle L_R(+t_p)H_{0,-t_p,-t_p} | L_R(+t_p) \rangle$ values in the $|R \uparrow(q_e,-t_p)\rangle$ and $|L \downarrow(q_e,-t_p)\rangle$ states are not zero, and opposite by each other, and the number of elements for color charge at time axis is two. On the other hand, the number of elements for color charge at space axis is one. Furthermore, there is only attractive forces between two or three color charges. Because of the $\langle L_R(+t_p)H_{0,-t_p,-t_p} | L_R(+t_p) \rangle$ terms, the color field only springs out from the infinitesimal source point to any direction in space and time axes. On the other hand, because of the $\langle R_L(+t_p)H_{0,-t_p,-t_p} | R_L(+t_p) \rangle$ terms, the color field only comes into the infinitesimal sink point from any direction in space and time axes. In summary,

because of the $\langle L_R(+t_p)H_{0,-t_p,-t_p} | L_R(+t_p) \rangle$ and $\langle R_L(+t_p)H_{0,-t_p,-t_p} | R_L(+t_p) \rangle$ terms, originating from the right- $|L_R(+t_p)\rangle$ and left- $|L_L(-t_p)\rangle$ handed helicity elements, and the left- $|R_L(+t_p)\rangle$ and right- $|R_R(-t_p)\rangle$ handed helicity elements, of the angular momentum in antiquark at the time axis, the color field springs out from the infinitesimal source point to any direction in time axis, or comes into the infinitesimal sink point from any direction in the time axis.

It should be noted that the strength of the color charge depends on time and the direction at the space axis. That is, the strength of the color charge can change, according to the time change and the spatial environment. This is because the color charge can be defined as the summation between the right- $\langle R_R(-t_p)H_{0,-t_p,-t_p} | R_R(-t_p) \rangle$ and left-handed $\langle R_L(+t_p)H_{0,-t_p,-t_p} | R_L(+t_p) \rangle$ angular elements and the left- $\langle L_L(-t_p)H_{0,-t_p,-t_p} | L_L(-t_p) \rangle$ and right-handed $\langle L_R(+t_p)H_{0,-t_p,-t_p} | L_R(+t_p) \rangle$ angular elements (time $t_p (\neq 0)$ dependent ($+t_p$ or $-t_p$)). That is, we can consider that the color charges are not rigid with respect to time change and the spatial environment. We can consider that the color charge observed in our real world can be defined as the summation of the angular momentum of the components of wave function for the right- (left-) handed particle and the right- (left-) handed antiparticle at particle time axis, as shown in Figs. 11 and 13. That is, we can consider that total color charges for antihadrons are always 0 (while) because each color charge for quarks and antiquarks can change with time so that the total energy for the environments for antihadrons can be minimum and stable (total while color charge). There is a possibility that even if each quarks and antiquarks could be separated, each quark or antiquark has zero color charge (i.e., green charge defined in this article), and thus we would not be able to observe the strong color charges (i.e., red and blue charges defined in this article). There is a possibility that the color charges for leptons and antileptons, which can be observed to be isolated, cannot be observed even if leptons and antileptons as well as the quarks and antiquarks have color charges.

If we observe the color charge for long enough time ($\Delta t \gg 0$), we would observe average $\varepsilon_{q_c,R,obs.\Delta t \gg 0}$ values originating from the both the $\langle R_R(-t_p)H_{0,-t_p,-t_p} | R_R(-t_p) \rangle$ and

$\langle R_L(+t_p)H_{0,-t_p,-t_p} | R_L(+t_p) \rangle$ terms, and from the both the $\langle L_L(-t_p)H_{0,-t_p,-t_p} | L_L(-t_p) \rangle$ and $\langle L_R(+t_p)H_{0,-t_p,-t_p} | L_R(+t_p) \rangle$ terms,

$$\varepsilon_{q_c, \mathbf{R}, \text{obs. } \Delta t \gg 0} = (2c_{R_R}^2 (q_e) - 1) \varepsilon_{q_{\infty}, \mathbf{R}}, \quad (125)$$

$$\varepsilon_{q_c, \mathbf{L}, \text{obs. } \Delta t \gg 0} = (2c_{L_L}^2 (q_e) - 1) \varepsilon_{q_{\infty}, \mathbf{L}}. \quad (126)$$

On the other hand, if we observe the color charge for short enough time ($\Delta t \approx 0$), we would observe various $\varepsilon_{q_c, \mathbf{R}, \text{obs. } \Delta t \approx 0}$ and $\varepsilon_{q_c, \mathbf{L}, \text{obs. } \Delta t \approx 0}$ values originating from only the $\langle R_R(-t_p)H_{0,-t_p,-t_p} | R_R(-t_p) \rangle$, or $\langle R_L(+t_p)H_{0,-t_p,-t_p} | R_L(+t_p) \rangle$, or other combinations between them, and from only the $\langle L_L(-t_p)H_{0,-t_p,-t_p} | L_L(-t_p) \rangle$, or $\langle L_R(+t_p)H_{0,-t_p,-t_p} | L_R(+t_p) \rangle$, or other combinations between them,

$$\begin{aligned} \varepsilon_{q_c, \mathbf{R}, \text{obs. } \Delta t \approx 0} &= \varepsilon_{q_{\infty}, \mathbf{R}} \\ &= \varepsilon_{q_{\infty}, \mathbf{L}} \\ &= \text{etc.} \end{aligned} \quad (127)$$

$$\begin{aligned} \varepsilon_{q_c, \mathbf{L}, \text{obs. } \Delta t \approx 0} &= \varepsilon_{q_{\infty}, \mathbf{L}} \\ &= \varepsilon_{q_{\infty}, \mathbf{R}} \\ &= \text{etc.} \end{aligned} \quad (128)$$

That is, if we observe the color charge for long enough time (i.e., the uncertainty of the time is very large ($\Delta t \gg 0$)), we would observe the average $\varepsilon_{q_c, \mathbf{R}, \text{obs. } \Delta t \gg 0}$ and $\varepsilon_{q_c, \mathbf{L}, \text{obs. } \Delta t \gg 0}$ values with very small uncertainty in energy ($\Delta E \approx 0$). On the other hand, if we observe the color charge in small enough time (i.e., the uncertainty of the time is very short ($\Delta t \approx 0$)), we would observe the various $\varepsilon_{q_c, \mathbf{R}, \text{obs. } \Delta t \approx 0}$ and $\varepsilon_{q_c, \mathbf{L}, \text{obs. } \Delta t \approx 0}$ values with very large uncertainty in energy ($\Delta E \gg 0$). This can be related to the Heisenberg's uncertainty principle. This is the reason why the gluon has the color charge energies ($\varepsilon_{q_c, \mathbf{R}, \text{ext.}}(q_e)$) as well as the strong force field energies ($\varepsilon_{q_c, \mathbf{R}, \text{int.}}(q_e)$), and the reason why the color charges and the number of gluons significantly change in hadrons and antihadrons with a time change.

7. Spin Magnetic Dipole Moment, Massive Charge, Electric Monopole Charge, and Color Charge in Particles and Antiparticles

Particles are composed from the wavefunction element for more dominant particle component traveling from the past to the future ($+t_p$) and for less dominant antiparticle component traveling from the future to the past ($-t_p$) at the particle time axis (t_p). In particles, the wavefunction element for the particle traveling from the past to the future ($+t_p$) is more dominant than that for antiparticle traveling from the future to the past ($-t_p$) at the particle time axis (t_p).

Antiparticles are composed from the wavefunction element for more dominant antiparticle component traveling from future to past ($-t_p$) and for less dominant particle component traveling from the past to the future ($+t_p$) at the particle time axis (t_p). In antiparticles, the wavefunction element for the antiparticle traveling from the future to the past ($-t_p$) is more dominant than that for the particle traveling from the past to the future ($+t_p$) at the particle time axis (t_p).

The q_g values for the particle are the same with those for their corresponding antiparticles. This is because the q_g values are not related to the time traveling axis.

The q_e values for the u , c , and t quarks (d , s , and b quarks) are $+2/3$ ($-1/3$) at the particle time axis. The q_e values for the e , μ , and τ leptons (ν_e , ν_μ , and ν_τ leptons) are -1 (± 0) at the particle time axis.

The q_e values for the u , c , and t quarks (d , s , and b quarks) are $-2/3$ ($+1/3$) at the antiparticle time axis. The q_e values for the e , μ , and τ leptons (ν_e , ν_μ , and ν_τ leptons) are $+1$ (± 0) at the antiparticle time axis.

The q_e values for the \bar{u} , \bar{c} , and \bar{t} antiquarks (\bar{d} , \bar{s} , and \bar{b} antiquarks) are $+2/3$ ($-1/3$) at the antiparticle time axis. The q_e values for the \bar{e} , $\bar{\mu}$, and $\bar{\tau}$ antileptons ($\bar{\nu}_e$, $\bar{\nu}_\mu$, and $\bar{\nu}_\tau$ antileptons) are -1 (± 0) at the antiparticle time axis.

The q_e values for the \bar{u} , \bar{c} , and \bar{t} antiquarks (\bar{d} , \bar{s} , and \bar{b} antiquarks) are $-2/3$ ($+1/3$) at the particle time axis. The q_e values for the \bar{e} , $\bar{\mu}$, and $\bar{\tau}$ antileptons ($\bar{\nu}_e$, $\bar{\nu}_\mu$, and $\bar{\nu}_\tau$ antileptons) are $+1$ (± 0) at the particle time axis.

The q_c values for the u , c , and t quarks (d , s , and b quarks) are Rd (Bl) at the particle time axis.

The q_c values for the u , c , and t quarks (d , s , and b quarks) are Bl (Rd) at the antiparticle time axis.

The q_c values for the \bar{u} , \bar{c} , and \bar{t} antiquarks (\bar{d} , \bar{s} , and \bar{b} antiquarks) are Rd (Bl) at the antiparticle time axis.

The q_c values for the \bar{u} , \bar{c} , and \bar{t} antiquarks (\bar{d} , \bar{s} , and \bar{b} antiquarks) are Bl (Rd) at the particle time axis.

The q_w values for the u , c , and t quarks (d , s , and b quarks) are $+1/2$ ($-1/2$) at the particle time axis. The q_w values for the e , μ , and τ leptons (ν_e , ν_μ , and ν_τ leptons) are $-1/2$ ($+1/2$) at the particle time axis.

The q_w values for the u , c , and t quarks (d , s , and b quarks) are $-1/2$ ($+1/2$) at the antiparticle time axis. The q_w values for the e , μ , and τ leptons (ν_e , ν_μ , and ν_τ leptons) are $+1/2$ ($-1/2$) at the antiparticle time axis.

The q_w values for the \bar{u} , \bar{c} , and \bar{t} antiquarks (\bar{d} , \bar{s} , and \bar{b} antiquarks) are $+1/2$ ($-1/2$) at the antiparticle time axis. The q_w values for the \bar{e} , $\bar{\mu}$, and $\bar{\tau}$ antileptons ($\bar{\nu}_e$, $\bar{\nu}_\mu$, and $\bar{\nu}_\tau$ antileptons) are $-1/2$ ($+1/2$) at the antiparticle time axis.

The q_w values for the \bar{u} , \bar{c} , and \bar{t} antiquarks (\bar{d} , \bar{s} , and \bar{b} antiquarks) are $-1/2$ ($+1/2$) at the particle time axis. The q_w values for the \bar{e} , $\bar{\mu}$, and $\bar{\tau}$ antileptons ($\bar{\nu}_e$, $\bar{\nu}_\mu$, and $\bar{\nu}_\tau$ antileptons) are $+1/2$ ($-1/2$) at the particle time axis.

Therefore, the antiquarks and antileptons at the antiquark space and time axes are equivalent to the quarks and leptons at the particle space and time axes. Furthermore, the physical parameters related to the time axis for the antiquarks and antileptons (quarks and leptons) are opposite to those for the quarks and leptons (antiquarks and antileptons) at the particle (antiparticle) space and time axes.

8. Ampère's Law

The right-handed $\langle \mathbf{R}_R(+k_p) \rangle_{H_{0,+k_p,+k_p}} | \mathbf{R}_R(+k_p) \rangle$ value at the space axis, denoting the right-handed magnetic field, is related to the right-handed $\langle \mathbf{R}_R(+t_p) \rangle_{H_{0,+t_p}} | \mathbf{R}_R(+t_p) \rangle$ value at the time axis, denoting the positive electric charge. This means that the right-handed magnetic field can be induced with respect to the traveling direction of the positively charged particle.

The left-handed $\langle \mathbf{L}_L(+k_p) \rangle_{H_{0,+k_p,+k_p}} | \mathbf{L}_L(+k_p) \rangle$ value at the space axis, denoting the left-handed magnetic field, is related to the left-handed $\langle \mathbf{L}_L(+t_p) \rangle_{H_{0,+t_p}} | \mathbf{L}_L(+t_p) \rangle$ value at the time axis, denoting the negative electric charge. This means that the left-handed magnetic field can be induced with respect to the traveling direction of the negatively charged

particle. This is the reason why we usually observe the Ampère's circuital law.

9. Small Gravitational Field

The $\varepsilon_{q_m, \mathbf{R}, \text{ext.}}(q_g)$ and $\varepsilon_{q_e, \mathbf{R}, \text{ext.}}(q_e)$ values are related to the diagonal $\langle \mathbf{R}_R(+k_p) \rangle_{H_{0,+k_p,+k_p}} | \mathbf{R}_R(+k_p) \rangle$ and $\langle \mathbf{R}_R(+t_p) \rangle_{H_{0,+t_p,+t_p}} | \mathbf{R}_R(+t_p) \rangle$ terms, respectively, and thus the cancellation of the right- and left-handed angular momentum is not significant. Therefore, the $\varepsilon_{q_m, \mathbf{R}, \text{ext.}}(q_g)$ and $\varepsilon_{q_e, \mathbf{R}, \text{ext.}}(q_e)$ values are not extremely small. The $\varepsilon_{q_e, \mathbf{R}, \text{ext.}}(q_e)$ values are related to the non-diagonal $\langle \mathbf{R}_R(+t_p) \rangle_{H_{1,+t_p,-t_p}} | \mathbf{R}_L(-t_p) \rangle$ terms at the time axis, and thus the cancellation of the right- and left-handed angular momentum can be significant. On the other hand, in the real world we live, the reversible process ($-t_p$) cannot be made in the time axis (irreversible). Therefore, we must consider the $\langle \mathbf{R}_R(+t_p) \rangle_{H_{0,+t_p}} | \mathbf{R}_R(+t_p) \rangle$ state instead of the $\langle \mathbf{R}_R(+t_p) \rangle_{H_{1,+t_p,-t_p}} | \mathbf{R}_L(-t_p) \rangle$ state. This (time traveling is irreversible) is the reason why the total chirality in the $\langle \mathbf{R}_R(+t_p) \rangle_{H_{0,+t_p}} | \mathbf{R}_R(+t_p) \rangle$ value in the $|\mathbf{R} \uparrow(q_e, +t_p)\rangle$ state is not zero, and the $\varepsilon_{q_e, \mathbf{R}, \text{ext.}}(q_e)$ value is not small. The $\varepsilon_{q_g, \mathbf{R}, \text{ext.}}(q_g)$ value is related to the non-diagonal $\langle \mathbf{R}_R(+t_p) \rangle_{H_{1,+t_p,-t_p}} | \mathbf{R}_L(-t_p) \rangle$ terms at the space axis, and thus the cancellation of the right- and left-handed angular momentum can be significant. In the real world we live, the reversible process ($-k_p$) can be possible in the space axis, and thus we can consider the $\langle \mathbf{R}_R(+t_p) \rangle_{H_{1,+t_p,-t_p}} | \mathbf{R}_L(-t_p) \rangle$ value. This is the reason why the $\varepsilon_{q_g, \mathbf{R}, \text{ext.}}(q_g)$ value is much smaller than the $\varepsilon_{q_m, \mathbf{R}, \text{ext.}}(q_g)$, $\varepsilon_{q_e, \mathbf{R}, \text{ext.}}(q_e)$, and $\varepsilon_{q_e, \mathbf{R}, \text{ext.}}(q_e)$ values.

Most of extremely large energy generated at the time of the Big Bang has been stored in the particle and antiparticle as a large potential rest energy $\varepsilon_{q_g, \mathbf{R}, \text{int.}}(q_g)$, and only small part of it is now used as very small gravitational energy $\varepsilon_{q_g, \mathbf{R}, \text{ext.}}(q_g)$. This is the reason why the gravity ($\varepsilon_{q_g, \mathbf{R}, \text{ext.}}(q_g)$) is much smaller than other three forces ($\varepsilon_{q_m, \mathbf{R}, \text{ext.}}(q_g)$, $\varepsilon_{q_e, \mathbf{R}, \text{ext.}}(q_e)$, and $\varepsilon_{q_e, \mathbf{R}, \text{ext.}}(q_e)$).

10. Concluding Remarks

In this research, we discussed the origin of the spin magnetic dipole moment, massive charge, electric monopole charge, and color charge for the particle and antiparticles at the particle and antiparticle spacetime axes.

Because of the $\langle R_R(+k_p)H_{0,+k_p,+k_p}|R_R(+k_p) \rangle$ and $\langle L_L(+k_p)H_{0,+k_p,+k_p}|L_L(+k_p) \rangle$ terms, originating from the finite right- and left-handed helicity elements, respectively, the magnetic dipole field goes from the infinitesimal source point to infinitesimal sink point at finite space axis. This is the reason why the path of the magnetic dipole field is like loop (source-sink)-type. The strength of the spin magnetic dipole moment depends on the direction at the space axis. That is, the strength of the spin magnetic dipole moment can change, according to the spatial environment. This is because the spin magnetic dipole moment can be defined as the difference between the diagonal right-handed $\langle R_R(+k_p)H_{0,+k_p,+k_p}|R_R(+k_p) \rangle$ and the diagonal left-handed $\langle L_L(+k_p)H_{0,+k_p,+k_p}|L_L(+k_p) \rangle$ angular momentum elements (space $k_p (\neq 0)$ dependent $(+k_p$ or $-k_p)$). That is, we can consider that the spin magnetic dipole moments are not rigid with respect to the spatial environment. We can consider that the spin magnetic dipole moment observed in our real world can be defined as the difference of the spin angular momentum between the components of wave function for the right- (left-) handed particle and the right- (left-) handed antiparticle. If we observe the magnetic dipole moment in large enough range and time (i.e., the uncertainty of the position and time is very large $(\Delta r \gg 0, t \gg 0)$), we would observe the average $\varepsilon_{q_m, R, obs. \Delta r, t \gg 0}$ and $\varepsilon_{q_m, L, obs. \Delta r, t \gg 0}$ values with very small uncertainty in momentum and energy $(\Delta k \approx 0, \Delta E \approx 0)$, as usual. On the other hand, if we observe the magnetic dipole moment in small enough range and time (i.e., the uncertainty of the position and time is very small $(\Delta r \approx 0, \Delta t \approx 0)$), we would observe the various $\varepsilon_{q_m, R, obs. \Delta r, t \approx 0}$ and $\varepsilon_{q_m, L, obs. \Delta r, t \approx 0}$ values with very large uncertainty in momentum and energy $(\Delta k \gg 0, \Delta E \gg 0)$. This can be related to the Heisenberg's uncertainty principle.

Because of the $\langle R_R(+k_p)H_{1,+k_p,-k_p}|R_L(-k_p) \rangle$ and $\langle L_L(+k_p)H_{1,+k_p,-k_p}|L_R(-k_p) \rangle$ terms, originating from the cancellation of the right- and left-handed helicity

elements at space axis, the gravitational fields only spring out from the infinitesimal source point (or comes into the infinitesimal sink point) to (from) any direction in the space axis. On the other hand, the total chirality and momentum in the $\langle R_R(+k_p)H_{1,+k_p,-k_p}|R_L(-k_p) \rangle$ and $\langle L_L(+k_p)H_{1,+k_p,-k_p}|L_R(-k_p) \rangle$ states are zero not because of the intrinsic zero value but because of the cancellation of the large right- and left-handed helicity elements, which are the origin of the spin magnetic moment and the electric charge. That is, we can consider that the gravity can be considered to be the residual electromagnetic forces. The strength of the massive charge is observed to be always constant, and not to depend on the direction at space axis. That is, the strength of the massive charge cannot change, according to the spatial environment. This is because the massive charge can be defined as the mixture (cancellation) of the right- and left-handed angular momentum elements at the space axis (at $k_{p, total} = (+k_p) + (-k_p) = 0$) (i.e., the non-diagonal $\langle R_R(+k_p)H_{1,+k_p,-k_p}|R_L(-k_p) \rangle$ and $\langle L_L(+k_p)H_{1,+k_p,-k_p}|L_R(-k_p) \rangle$). That is, we can consider that the massive charges are rigid with respect to the spatial environment. We can consider that the massive charge observed in our real world can be defined as the mixture (cancellation) of the components of angular momentum wave function for the right- (left-) handed particle and the right- (left-) handed antiparticle at space axis (at $k_{p, total} = (+k_p) + (-k_p) = 0$).

Because of the $\langle R_R(+t_p)H_{1,+t_p,-t_p}|R_L(-t_p) \rangle$ and $\langle L_L(+t_p)H_{1,+t_p,-t_p}|L_R(-t_p) \rangle$ terms, originating from the mixture of the right- and left-handed helicity elements, the electric field springs out from the infinitesimal source point to any direction in the time axis, or comes into the infinitesimal sink point from any direction in the time axis. The strength of the electric monopole charge is observed to be always constant at time axis, and not to depend on the direction at space axis. That is, the strength of the electric monopole charge cannot change, according to the spatial and time environment. This is because the electric monopole charge can be defined as the mixture (cancellation) of the right- and left-handed angular momentum elements at the time axis (at $t_{p, total} = (+t_p) + (-t_p) = 0$) (i.e., the non-diagonal $\langle R_R(+t_p)H_{1,+t_p,-t_p}|R_L(-t_p) \rangle$ and

$\langle L_L(+t_p) | H_{1,+t_p,-t_p} | L_R(-t_p) \rangle$). That is, we can consider that the electric monopole charges are rigid with respect to the spatial and time environment. We can consider that the electric monopole charge observed in our real world can be defined as the mixture (cancellation) of the components of angular momentum wave function for the right- (left-) handed particle and the right- (left-) handed antiparticle at the time axis. We can interpret that the electric monopole charges are generated by the virtual particle-antiparticle pair annihilation interaction in a particle (at $k_{p,\text{total}} = (+k_p) + (+k_a) = 0$, at $t_{p,\text{total}} = (+t_p) + (+t_a) = 0$).

Because of the $\langle R_R(+t_p) | H_{0,+t_p,+t_p} | R_R(+t_p) \rangle$ and $\langle L_L(+t_p) | H_{0,+t_p,+t_p} | L_L(+t_p) \rangle$ terms, originating from the right- $|R_R(+t_p)\rangle$ and left- $|R_L(-t_p)\rangle$ handed helicity elements, and the left- $|L_L(+t_p)\rangle$ and right- $|L_R(-t_p)\rangle$ handed helicity elements, of the angular momentum in quark at the time axis, the color field springs out from the infinitesimal source point to any direction in time axis, or comes into the infinitesimal sink point from any direction in the time axis. The strength of the color charge depends on time and the direction at the space axis. That is, the strength of the color charge can change, according to the time change and the spatial environment. This is because the color charge can be defined as the summation between the diagonal right- $\langle R_R(+t_p) | H_{0,+t_p,+t_p} | R_R(+t_p) \rangle$ and left-handed $\langle R_L(-t_p) | H_{0,+t_p,+t_p} | R_L(-t_p) \rangle$ angular elements, and the diagonal left- $\langle L_L(+t_p) | H_{0,+t_p,+t_p} | L_L(+t_p) \rangle$ and right-handed $\langle L_R(-t_p) | H_{0,+t_p,+t_p} | L_R(-t_p) \rangle$ angular elements (time $t_p (\neq 0)$ dependent $(+t_p$ or $-t_p)$). That is, we can consider that the color charges are not rigid with respect to time change and the spatial environment. We can consider that the color charge observed in our real world can be defined as the summation of the angular momentum of the components of wave function for the right- (left-) handed particle and the right- (left-) handed antiparticle at particle time axis. That is, we can consider that total color charges for hadrons are always 0 (while) because each color charge for quarks and antiquarks can change with time so that the total external energy for the environments for hadrons can be minimum and stable (total while color charge). If we observe the color charge for long enough time (i.e., the uncertainty of the time is

very large ($\Delta t \gg 0$)), we would observe the average $\varepsilon_{q_c, R, \text{obs.} \Delta t \gg 0}$ and $\varepsilon_{q_c, L, \text{obs.} \Delta t \gg 0}$ values with very small uncertainty in energy ($\Delta E \approx 0$). On the other hand, if we observe the color charge in small enough time (i.e., the uncertainty of the time is very short ($\Delta t \approx 0$)), we would observe the various $\varepsilon_{q_c, R, \text{obs.} \Delta t \approx 0}$ and $\varepsilon_{q_c, L, \text{obs.} \Delta t \approx 0}$ values with very large uncertainty in energy ($\Delta E \gg 0$). This can be related to the Heisenberg's uncertainty principle. This is the reason why the gluon has the color charge energies ($\varepsilon_{q_c, R, \text{ext.}}(q_c)$) as well as the strong force field energies ($\varepsilon_{q_c, R, \text{int.}}(q_c)$), and the reason why the color charges and the number of gluons significantly change in a hadron with a time change.

Acknowledgments

This work is supported by The Iwatani Naoji Foundation's Research Grant.

References

- [1] T. Kato, "Diamagnetic currents in the closed-shell electronic structures in sp³-type hydrocarbons" Chemical Physics, vol. 345, 2008, pp. 1–13.
- [2] T. Kato, "The essential role of vibronic interactions in electron pairing in the micro- and macroscopic sized materials" Chemical Physics, vol. 376, 2010, pp. 84–93.
- [3] T. Kato, "The role of phonon- and photon-coupled interactions in electron pairing in solid state materials" Synthetic Metals, vol. 161, 2011, pp. 2113–2123.
- [4] T. Kato, "New Interpretation of the role of electron-phonon interactions in electron pairing in superconductivity" Synthetic Metals, vol. 181, 2013, pp. 45–51.
- [5] T. Kato, "Relationships between the intrinsic properties of electrical currents and temperatures" Proceedings of Eleventh TheIIER International Conference, February 2015, Singapore, pp. 63–68.
- [6] T. Kato, "Relationships between the nondissipative diamagnetic currents in the microscopic sized atoms and molecules and the superconductivity in the macroscopic sized solids" Proceedings of Eleventh TheIIER International Conference, February 2015, Singapore, pp. 69–80.
- [7] T. Kato, "Vibronic stabilization under the external applied fields" Proceedings of Eleventh TheIIER International Conference, February 2015, Singapore, pp. 110–115.
- [8] T. Kato, K. Yoshizawa, and K. Hirao, "Electron-phonon coupling in negatively charged acene- and phenanthrene-edge-type hydrocarbons" J. Chem. Phys. vol. 116, 2002, pp. 3420-3429.

[9] R. Mitsuhashi, Y. Suzuki, Y. Yamanari, H. Mitamura, T. Kambe, N. Ikeda, H. Okamoto, A. Fujiwara, M. Yamaji, N. Kawasaki, Y. Maniwa, and Y. Kubozono, “Superconductivity in alkali-metal-doped picene” *Nature* vol. 464, 2010, pp. 76-79.

[10] T. Kato, “Electronic Properties under the External Applied Magnetic Field in the Normal Metallic and Superconducting States” *Int. J. Sci. Eng. Appl. Sci.*, vol. 1, Issue 7, 2015, pp.300-320.

[11] T. Kato, “Electron–Phonon Interactions under the External Applied Electric Fields in the Normal Metallic and Superconducting States in Various Sized Materials” *Int. J. Sci. Eng. Appl. Sci.*, vol. 1, Issue 8, 2015, pp.1-16.

[12] M. Murakami, Chodendo Shin-Jidai (meaning “New Era for Research of Superconductivity”), Kogyo-Chosakai, Tokyo, 2001 (in Japanese).

[13] T. Kato, “Relationships between the Electric and Magnetic Fields” *Int. J. Sci. Eng. Appl. Sci.*, vol. 1, Issue 9, 2015, pp.128-139.

[14] T. Kato, “Unified Interpretation of the Gravitational, Electric, Magnetic, and Electromagnetic Forces” *Int. J. Sci. Eng. Appl. Sci.*, vol. 2, Issue 1, 2016, pp.153-165.

[15] T. Kato, “Relationships between the Electromagnetic and Strong Forces” *Int. J. Sci. Eng. Appl. Sci.*, vol. 2, Issue 2, 2016, pp.119-134.

[16] T. Kato, “Higgs Mechanism in Superconductivity and Weak Interactions” *Int. J. Sci. Eng. Appl. Sci.*, vol. 2, Issue 3, 2016, pp.148-170.

[17] S. Asai, Higgs-Ryushi No Nazo (meaning “Mystery of Higgs Particle”), Shoden-Sha, Tokyo, 2012 (in Japanese).

2013, *The Nikkei*; (3) November 7, 2011, *The Nikkei*; (4) January 14, 2011, *The Nikkei*; (5) November 22, 2010, *The Nikkei*; (6) November 18, 2010, *The Nikkei*).

Author Profile

Dr. Takashi Kato is a Professor at Nagasaki Institute of Applied Science, Japan. He completed his doctorate in physical chemistry with the theory of vibronic interactions and Jahn–Teller effects at Kyoto University (PhD (Engineering)), Japan, in 2000. During October 2001–February 2003, he has performed research concerning prediction of the occurrence of superconductivity of graphene-like aromatic hydrocarbons such as phenanthrene, picene, and coronene at Max-Planck-Institute for Solid State Research in Stuttgart, Germany, as a visiting scientist. In 2010, his prediction of the occurrence of superconductivity of picene and coronene were experimentally confirmed at Okayama University, Japan, and in 2011, that of phenanthrene was experimentally confirmed at University of Science and Technology of China. His theory and calculations concerning the guiding principle towards high-temperature superconductivity are highly regarded and recently reported several times in newspaper (*The Nikkei*), which is the most widely read in Japan, as follows ((1) July 8, 2014, *The Nikkei*; (2) October 19,